YAP1 Oncogene is a Context-specific Driver for Pancreatic Ductal Adenocarcinoma

Bo Tu[1], Jun Yao[1], Sammy Ferri-Borgogno[2,3], Jun Zhao[2], Shujuan Chen[1], Qiuyun Wang[1], Liang Yan[1], Xin Zhou[1,8], Cihui Zhu[1], Seungmin Bang[9], Qing Chang[4], Christopher A. Bristow[4], Ya'an Kang[5], Hongwu Zheng[10], Huamin Wang[2], Jason B. Fleming[5,11], Michael Kim[5], Giulio F. Draetta[1,6], Duojia Pan[12], Anirban Maitra[2,3], Wantong Yao[6,7*], Sonal Gupta[2,3*], Haoqiang Ying[1*]

[1]Departments of Molecular and Cellular Oncology, [2]Department of Pathology, [3]Sheikh Ahmed Center for Pancreatic Cancer Research, [4]Institute for Applied Cancer Science, [5]Department of Surgical Oncology, [6]Department of Genomic Medicine, [7]Department of Translational Molecular Pathology, University of Texas MD Anderson Cancer Center, Houston, Texas; [8]Department of Obstetrics and Gynecology, Shengjing Hospital, China Medical University, Shenyang, Liaoning, China; [9]Department of Internal Medicine, Institute of Gastroenterology, Yonsei University College of Medicine, Seoul, Korea; [10]Department of Pathology and Laboratory Medicine, Weill Cornell Medical College, New York City, New York; [11]Department of Gastrointestinal Oncology, Moffitt Cancer Center, Tampa, Florida; [12]Department of Physiology, Howard Hughes Medical Institute, University of Texas Southwestern Medical Center, Dallas, Texas.

***Corresponding Authors:** Wantong Yao, PhD, Department of Translational Molecular Pathology, The University of Texas MD Anderson Cancer Center, 2130 West Holcombe Blvd., Houston, TX 77030, USA; Phone: 713-792-6803, Email: wyao2@mdanderson.org. Sonal Gupta, PhD, Department of Pathology, The University of Texas MD Anderson Cancer Center, 6565 MD Anderson Blvd., Houston, TX 77030, USA; Phone: 713-745-0831, Email: sgupta8@mdanderson.org. Haoqiang Ying, MD, PhD, The University of Texas MD Anderson Cancer Center, 1515 Holcombe Blvd., Houston, TX 77030, USA, Phone: 713-563-3367, Email: hying@mdanderson.org.

Author Contributions: B.T., W.Y., S.F-B., S.C., Q.W., L.Y., X.Z. and S.G. performed data collection and interpretation. J.Y., provided statistical and bioinformatics analysis. C.Z. and S.B. contributed to animal breeding. Q.C., C.B., Y.K., H.Z., H.W., J.F. and M.K. provided clinical specimen and data analyses on PDX samples. J.Z., H.W. and A.M. performed pathology analyses. G.D., D.P. and A.M. provided crucial feedback on manuscript. W.Y., S.G. and H.Y. drafted the manuscript. W.Y., S.G. and H.Y. did conception, design and supervision of the study.

Word count: 8230

Significance of this study

What is already known on this subject?

- Pancreatic ductal adenocarcinoma (PDAC) is recently classified into distinct molecular subtypes with the squamous subtype correlated with worst prognosis.
- The molecular subtypes of PDAC are based on gene expression and are not consistently associated with any genetic alterations, such as KRAS mutations.
- YAP1 oncogene is required for oncogenic KRAS-induced PDAC development.
- YAP1 amplification in genetically engineered mouse model of PDAC enables the bypass of KRAS-dependency.

What are the new findings?

- YAP1 is highly activated in squamous subtype PDAC and is required for tumorigenic activity.
- YAP1 activation in squamous subtype PDAC is mediated by WNT5A overexpression.
- WNT5A overexpression in PDAC tumor cells bypasses KRAS-dependency.

How might it impact on clinical practice in the foreseeable future?

- YAP1 activation signature may serve to stratify PDAC patients for YAP1 targeted therapy.
- The WNT5A-YAP1 axis can serve as therapeutic target for squamous subtype PDAC with WNT5A overexpression and YAP1 activation.
- Tumors with YAP1 activation may quickly develop resistance to KRAS targeted therapy.

Abstract

Objective: *Yap1* oncogene is essential for KRAS-induced pancreatic ductal adenocarcinoma (PDAC) initiation. We recently demonstrated that YAP1 is capable of bypassing KRAS-dependency. However, genetic alterations of YAP1 pathway are rare in human PDAC and its role in tumor maintenance remains unclear. This study investigates YAP1 function in transcriptionally distinct subsets of PDAC and explores the molecular mechanisms for YAP1 activation.

Design: Conditional *Yap1* allele was crossed into *LSL-Kras*$^{G12D/+}$; *Trp53*$^{R172H/+}$; *Mist1-Cre*$^{ERT2+}$ mice to study the requirement of *Yap1* for PDAC development in adult mice. YAP1 function in advanced PDAC was analyzed in human tissues, PDAC cell lines, patient-derived xenograft samples and mouse PDAC cells, using in vitro and in vivo assays and gene expression analyses. WNT5A expression and its effect on YAP1 activation as well as tumorigenic activity was studied in aforementioned human and mouse systems using genetic and pharmacological approaches. The bypass of KRAS-dependency by WNT5A was evaluated in *Kras*^{G12D}-driven mouse PDAC cells.

Results: *Yap1* deletion blocked *Kras*^{G12D}/*Trp53*$^{R172H/+}$ induced PDAC development in mice. YAP1 activation correlated with squamous subtype of human PDAC and poor prognosis. YAP1 activation enhanced malignant phenotype and YAP1 depletion suppressed the tumorigenic activity specifically in squamous subtype tumors. WNT5A was significantly overexpressed in squamous subtype tumors and positively correlated with YAP1 activity. Conversely, WNT5A depletion resulted in YAP1 inactivation and inhibition of tumorigenic activity. WNT5A expression enabled cell survival and tumor growth in the absence of oncogenic *Kras*.

Conclusions: YAP1 oncogene is a major driver for squamous subtype PDAC whose activation is mediated by WNT5A overexpression.

Introduction

Pancreatic ductal adenocarcinoma, expected to become the second most common cause of cancer-related mortality in the US by 2030[1], is a highly heterogeneous disease with complex genetic and molecular diversity. While majority of PDACs share near-ubiquitous oncogenic mutations of *KRAS* and the frequent inactivation of *TP53*, *SMAD4* and *CDKN2A* tumor suppressors, most additional somatic mutations occur at low individual prevalence, suggesting diverse mechanisms underlying PDAC progression[2]. Although others and we have shown that *KRAS* oncogene is essential for tumor maintenance[3] [4], effective targeting of KRAS pathway is yet to be achieved clinically. Moreover, recent studies have revealed a subpopulation of PDAC cells may bypass KRAS-dependency in advanced tumors[5-7], pointing to a critical need to identify context-specific vulnerabilities to improve patient outcome.

Recent large-scale molecular analyses have confirmed that human PDAC can be classified into several subtypes based on transcriptome profiles[8-11]. Although the subtype nomenclature varies between individual reports, the molecular signature of each subtype is largely overlapping across these studies. Since it has been suggested that the expression signatures of some of the subtypes, such as ADEX/exocrine or immunogenic subtype, are likely derived from non-neoplastic cells[9 11], the molecular signatures of tumor cells largely fall into two categories, namely the squamous/quasimesenchymal/basal-like and the progenitor/classical subtypes. Although the expression subtypes are not consistently associated with any somatic mutation or other genetically altered pathways[11], the squamous subtype reproducibly exhibits worse prognosis compared to other subtypes[8 10 11]. This suggest the biological phenotype of these tumor subgroups are driven by subtype-specific molecular mechanisms other than genetic alterations and thus, identifying the oncogenic pathways that drive the squamous subtype tumors will reveal subtype-specific vulnerabilities to treat these highly malignant tumors.

Yes-associated protein 1 (YAP1) is a transcriptional coactivator and plays critical roles in controlling tissue growth during organ development[12]. Its activity is kept in check by the upstream Hippo pathway, composed of the MST1/2-LATS1/2 kinases cascade, which phosphorylates YAP1 at multiple serine residues and sequesters YAP1 in cytoplasm for degradation[13]. Recent studies showed that YAP1 activation is commonly observed in tumor cells and in vivo studies using genetically engineered mouse (GEM) models have shown that hyper-activation of YAP1 results in acinar-to-ductal metaplasia, a trans-differentiation process tightly correlated with PDAC initiation[14 15]. Conversely, pancreas-specific *Yap1* deletion in GEM models abolished PDAC development driven by oncogenic *Kras*, suggesting YAP1 is essential for tumor initiation[16 17]. Recent studies also indicate that YAP1 activation is associated with more aggressive behavior of PDAC such as epithelial-to-mesenchymal transition (EMT) and liver metastasis [18 19]. In addition, we recently showed that *Yap1* amplification is sufficient to bypass KRAS dependency in an inducible PDAC GEM model[5], implicating YAP1 may substitute oncogenic KRAS to sustain tumor growth. However, the requirement for YAP1 in tumor maintenance in advanced human PDAC is yet to be thoroughly verified. Though, YAP1 is activated in human PDAC[16 20], the mechanisms that lead to YAP1 activation in PDAC cells remain largely elusive. Here we show that YAP1 is not only required for PDAC initiation in adult animals, but also remains activated in a subset of advanced human PDACs with squamous subtype feature and is required for their tumorigenic activity. We further identify WNT5A overexpression as one of the mechanisms leading to YAP1 activation in the deadliest form of PDAC.

Material and Methods

Transgenic Mice

For generation of tamoxifen-inducible PDAC GEM model, *Mist1*$^{Cre\text{ERT2}/+}$ [21] mice were used for conditional activation of mutant *Kras*^{G12D} and mutant *Trp53*^{R172H} in the mature pancreas. For *Yap1* deletion, these mice were further crossed with *Yap1*$^{fl/fl}$ mice[22]. For most efficient recombination, tamoxifen was

administered (i.p.) to 6-week old mice in corn oil once daily for 5 days. The recombination efficiency was tested using PCR primers designed specifically to detect wildtype and recombinant alleles of *Kras*, *Trp53* and *Yap1* in pancreatic tissue. All manipulations were approved under MD Anderson Cancer Center (MDA) Institutional Animal Care and Use Committee (IACUC) under protocol number 00001549.

Xenograft Studies

All xenograft studies were carried out in NCr nude mice (Taconic) and were approved by the MD Anderson IACUC under protocol number 00001549. Details for the xenograft studies are described in Supplementary Methods.

Cell Culture and Establishment of Primary PDAC lines

Human pancreatic cell lines SNU410, HPAC, HPAFII, PL45, PaTu8988S and PaTu8988T were obtained from ATCC. Pa04C was established from resected patient tumors and maintained as low passage (<10)[23] and cultured according to recommended protocols. Establishment and maintenance of primary mouse PDAC lines was performed as described previously [4 5]. Mouse PDAC cell line, PD3077, was gift from Dr. Ben Stanger, University of Pennsylvania Perelman School of Medicine. The human patient PDX cell lines were maintained in RPMI-1640 medium containing 10% FBS (Clontech). KRAS mutation status, molecular subtypes and tumor grade information are listed in Supplementary Table 1.

Reagents

Doxycycline (RPI), PE Annexin V Apoptosis Detection Kit I (BD Biosciences), BOX5 (EMD Millipore).

Immunostaining and Western Blot Analysis

Immunohistochemical (IHC) analysis was performed as described earlier[24]. Details for immunofluorescence staining, western blot and primary antibody information are described in Supplementary Methods.

Lentivirus Mediated shRNA Knockdown

All lentiviral shRNA clones targeting YAP1, WNT5A and non-targeting shRNA control were obtained from Sigma Aldrich in the pLKO vector. The clone IDs for the shRNA are listed in Supplementary Materials.

Crispr-Cas9 Mediated Gene Knockout (KO)

sgRNAs targeting mouse *Wnt5a* or *Yap1* were cloned into pSpCas9(BB)-2A-Puro (Addgene, #62988) and transfected into target cells. After 2 μg/ml puromycin selection for 1 week, single cell clones are isolated and analyzed by T7E1 assay and Western blot. Sequences for *Wnt5a* and *Yap1* sgRNA are listed in Supplementary Materials.

TMA staining and analysis

Immunohistochemical staining for YAP1 was performed on 5-μm unstained sections from the tissue microarray blocks, which included 92 (MD Anderson Cancer Center (MDA)) or 83 (Johns Hopkins University School of Medicine (JHU)) PDAC samples from patients who underwent upfront surgery. The immunohistochemical staining for YAP1 was reviewed by a pathologist (H.W.). The expression of YAP1 was classifies as YAP1-low and YAP1-high using the median score for total YAP1 expression (nuclear plus cytoplasmic expression) as a cutoff.

Statistical Analysis

Tumor volume and tumor free survivals were analyzed using GraphPad Prism. To assess distributional differences of variance across different test groups, the Mann-Whitney test was used. Other comparisons were performed using the unpaired Student t-test. For all experiments with error bars, standard deviation (SD) was calculated to indicate the variation with each experiments and data, and values represent mean ± SD.

Results

YAP1 is required for PDAC development in adult mice

To evaluate the role of YAP1 in human PDAC, tissue microarray (TMA) analysis in a cohort of 92 human PDAC showed that 47% PDACs exhibit high YAP1 protein expression in tumor epithelium compared to surrounding stromal tissue. The median overall survival (OS) for YAP1-low group was 38.3 months compared to 25.3 months for YAP1-high group (p=0.02) (Fig.1A&B). Such association between elevated YAP1 protein and poor survival was further validated in an independent cohort of 83 PDAC patients (p=0.0475) (Fig.1C), implicating YAP1 may promote adverse biological outcomes in PDAC. The in vivo function of YAP1 during PDAC development was further characterized using genetically engineered mouse (GEM) models. Previous studies have shown that conditional *Yap1* deletion at early embryonic stage blocked mutant *KRAS*-driven initiation of acinar to ductal metaplasia (ADM), premalignant lesions and subsequent tumor formation in GEM models[16 17]. To more faithfully recapitulate the PDAC initiation of human patients, we investigated the requirement of YAP1 for PDAC when the tumor initiation is started in adult pancreas. Tamoxifen-induced acinar-specific activation of Cre recombinase in adult pancreas of the *Mist1-Cre*^{ERT2}; *LSL-Kras*$^{G12D/+}$; *LSL-Trp53*$^{R172H/+}$ (MKP) model leads to rapid PDAC development accompanied by induction of nuclear YAP1 expression in tumor cells (Fig. 1D, *left*, YAP-WT). In contrast, acinar-specific deletion of *Yap1* in the MKPY (YAP-KO) model completely blocked tumor development, resulting in relatively normal pancreas (Fig.1D-F). While all MKP mice succumbed to PDAC with a median survival of 103 days (n=29), *Yap1*-null MKPY mice remained entirely free of any overt disease and pathological lesion (n=29) (Fig.1G). This could be attributed to the effect of YAP1 on cell proliferation and survival, as evident by loss of both Ki67 and survivin (BIRC5) staining in YAP-KO pancreas (Fig.1H & S1A). The protective effect of *Yap1* deletion on *Kras*^{G12D} and *Trp53*$^{R172H/+}$ -induced PDAC development was further confirmed with an independent tamoxifen-inducible *Elastase-Cre*^{ERT2}; *LSL-Kras*$^{G12D/+}$; *LSL-Trp53*$^{R172H/+}$ model (Fig.S1B).

YAP1 is activated in squamous subtype of human PDAC

Gain-of-function studies showed that ectopic expression of mutant YAP1^{S127A}, a constitutively active YAP1 resistant to cytoplasmic retention and degradation [13], drastically enhanced the anchorage-independent growth, migration and invasion capacity of human PDAC cell line PaTu8988S cells and Pa04C cells, an early passage patient-derived cell line (Fig.2A-C, S2A), suggesting active YAP1 may promote the tumorigenicity and metastatic spread of PDAC cells. Indeed, YAP1^{S127A} expression diminished necrotic regions within primary tumor core and enhanced the distal metastasis of Pa04C cells in an orthotopic xenograft model (Fig.2D&E, S2B-C). This was accompanied by induction of canonical YAP1 target genes, such as *CYR61*, *CTGF* and *AXL* in both cultured cells and xenograft tumors (Fig.S2D&E), suggesting YAP1 activation contributing to this aggressive phenotype. Gene expression microarray and subsequent Gene Set Enrichment Analysis (GSEA) in these cells confirmed an established YAP1 signature (Fig.S2F), enrichment in pathways associated with tumor development and metastasis, and the underlying cellular processes responsible, such as cell proliferation, cell cycle progression, migration, motility and EMT (Supplementary Tables 2-3). By QPCR, we also confirmed upregulation of several genes reported to be involved in EMT in Pa04C-YAP^{S127A} tumors (Fig.S2E). Interestingly, cellular processes like cell cycle progression and signaling pathways significantly activated in Pa04C-YAP1^{S127A} such as MYC, IL6-STAT3, TGFβ, RhoA, E2F, TNF etc., along with Hippo signaling pathway were part of all four gene signatures (GP2-5) associated with squamous subtype of PDAC[8] (Supplementary Table 4-5), implicating the role of YAP1 activation in this most aggressive subtype.

To address this, we analyzed the expression profiles of human PDAC from the recent ICGC collection[8] and found that tumors of squamous subtype exhibit elevated expression of genes that are known to be associated with YAP1 activation[25] (Fig.2F&G, Supplementary Table 6). Moreover, the expression of YAP1 activation signature is significantly correlated with that of the squamous subtype signature in both TCGA and ICGC datasets (Fig.2H), underscoring the tight relationship between YAP1

activation and squamous subtype tumors. YAP1 pathway activation is significantly correlated with poor survival in PDAC patients (Fig.2I). Squamous subtype has also been shown to be associated with poor prognosis[8 10]. Thus, to exclude the possibility that correlation between YAP1 activation and shortened patient survival is merely a reflection of enrichment of YAP1 signature in squamous subtype, we further analyzed the prognostic value of YAP1 signature in PDAC subtypes other than the squamous subtype. Indeed, the median patient survival significantly declines with the increase of YAP1 activation signature in those non-squamous subtype tumors (Fig.2J), indicating that YAP1 pathway activation is an independent prognosis factor in PDAC patients.

To further exclude the possibility that YAP1 activation signature in squamous subtype PDAC is largely derived from tumor stroma, we analyzed the transcriptome data of human PDAC cell lines from CCLE dataset and that of a collection of 47 PDAC PDX models, after the expression reads from murine host were omitted. We failed to identify cell lines or PDX models that are enriched with ADEX or immunogenic signatures (Fig.S2G&H, and data not shown), consistent with the notion that the molecular signatures of these subtypes are likely derived from non-tumor cells[9]. Not surprisingly, the molecular signatures of human PDAC cell lines or PDXs mostly clustered under either progenitor or squamous subtype (Fig. S2G&H). In accordance with the analysis of ICGC data, YAP1 activation signature was consistently elevated in squamous subtype (Fig.2K&L). Interestingly, multiplexed gene expression analysis using the NanoString platform showed that, in contrast to the parental PaTu8988S cells that belonged to progenitor subtype, the molecular signature of PaTu8988S cells expressing YAP1^{S127A} was highly similar to that of PaTu8988T cells, which were derived from the same patient as PaTu8988S cells[26] but of squamous subtype (Fig.S2I, Supplementary Table 7). The induction of squamous subtype by YAP1 activation is further verified in vivo where the Pa04C-YAP^{S127A} tumors exhibited induction of squamous

subtype gene expression and suppression of progenitor subtype gene expression (Fig.S2J). Together, our data indicates that YAP1 activation is capable of driving the molecular signature of squamous subtype.

YAP1 is essential for the maintenance of squamous subtype PDACs

To further investigate the requirement of YAP1 in squamous subtype PDAC, we conducted loss-of-function studies with shRNA in a panel of human PDAC cell lines and early-passage primary cell lines derived from human PDX tumors. Knockdown of YAP1 strongly suppressed the colony formation capacity of PDAC cell lines (PaTu8988T, SNU410 and PL45) and PDX lines (PATC148 and PATC153) belonging to squamous subtype with strong YAP1 activation signature (Fig.3A-D, S2G-H). In contrast, progenitor subtype cell lines with low YAP1 signature, including PaTu8988S, HPAF-II, HPAC PATC102 and PATC108 cells, were less sensitive to YAP1 depletion (Fig.3A-D, S2G-H). Moreover, inducible knockdown of YAP1 in established tumors induced regression in PaTu8988T tumors while the growth of PaTu8988S tumors were not affected (Fig.S3A-B), indicating the role of YAP1 for tumor maintenance in squamous subtype PDAC.

Others and we have previously showed that YAP1 activation enables the bypass of oncogene addiction in multiple cancer types, including PDAC[5] [27-29]. Indeed, compared to PaTu8988S cells, PaTu8988T cells were more resistant to KRAS knockdown with shRNA (Fig.3E-F&S3C). Expression of YAP1^{S127A} partially rescued the growth of PaTu8988S cells upon KRAS depletion (Fig.3E-F&S3C), indicating that YAP1 activation could enable bypass of KRAS-dependence in PDAC cells. Accordingly, pathway analysis of human PDAC expression profiles in the ICGC dataset indicated that gene signatures induced upon KRAS knockdown [30] or suppressed by oncogenic KRAS expression [31] were significantly upregulated in squamous subtype tumors (Fig.S3D), implying relatively low KRAS activity in these tumors. By using an inducible *Kras*^{G12D}-driven PDAC GEM model, we have recently obtained a collection of spontaneous relapse tumors following *Kras*^{G12D} extinction in advanced PDAC (iKras- tumors)[5]. These

tumors neither expressed oncogenic *Kras* nor exhibited strong activation of KRAS surrogates, and are thus deemed as KRAS-independent. Interestingly, molecular signature of the iKras- tumors (Supplementary Table 8), which is composed of genes that highly expressed in iKras- tumors compared to iKras+ tumors [5], was also significantly enriched in squamous subtype of human PDACs (Fig.3G&S3E), further supporting the notion that squamous subtype tumors are relatively KRAS-independent. Consistent with the YAP1 activation in human squamous subtype PDAC, YAP1 signature is significantly enriched in the mouse iKras- tumors (Fig.3H). While YAP1 knockdown exhibit minimal effect on progenitor subtype *Kras*-driven mouse tumor lines (AK192 and 19636) [4 5], YAP1 depletion significantly suppressed the proliferation and colony formation capability of squamous subtype cells (PD3077) [32] and iKras- tumor cells (Fig.3I-J, S3F), underscoring the YAP1 dependency in squamous subtype tumors. Interestingly, re-induction of $KRAS^{G12D}$ expression with doxycycline in iKras- cells fails to sustain colony formation following YAP1 knockdown (Fig.S3G-I), suggesting YAP1 activation may render oncogenic KRAS obsolete in PDAC cells.

WNT5A overexpression contributes to YAP1 activation in PDAC

In an effort to identify mechanism for YAP1 activation, genomic analysis of primary human tumors from ICGC or TCGA dataset didn't reveal frequent copy number changes or mutations of *YAP1* locus (Fig.S4A). While *Yap1* is amplified in a subset of mouse iKras- tumors[5], most iKras- tumors harbor no genomic alteration of *Yap1* despite enrichment of YAP1 signature (Fig. 3H&S4B), indicating non-genetic mechanisms cause YAP1 activation in PDAC. In addition, no obvious difference in YAP1 transcription level was observed between squamous and progenitor subtype PDAC cell lines (Fig. S4C). YAP1 activation occurs by its nuclear translocation [13], which indeed, was evident in YAP1-dependent human PDAC cells, including PaTu8988T, SNU410 and PL45 cells, and iKras- mouse tumors or the derived cell lines without *Yap1* amplification (*iKras- Yap1*$^{Amp-}$) (Fig.4A&B, S4D). Conversely, YAP1 was

localized in both cytoplasm and nuclei in PDAC cells with weak YAP1 signature, such as PaTu8988S, HPAF-II and HPAC cells, as well as progenitor subtype *Kras*^{G12D}-driven mouse tumors and iKras- tumors with *Yap1* amplification (*iKras- Yap1*$^{Amp+}$) (Fig.4A&B). Accordingly, YAP1 activated human and mouse PDAC cells exhibit reduced phosphorylation at S127, the target site for directly upstream LATS1/2 kinases, along with corresponding trend of decrease in LATS1/2 phosphorylation, an indicator of LATS1/2 activity (Fig.S4E-H). Surprisingly, no obvious difference was observed for MST1/2 phosphorylation or their total protein level (Fig.S4E-H), suggesting YAP1 activation in PDAC cells may through direct modulation of LATS1/2 activity, independent of MST1/2.

To identify the mechanisms leading to YAP1 activation, we compared the differentially regulated pathways in *iKras- Yap1*$^{Amp-}$ vs *iKras- Yap1*$^{Amp+}$ cells with GSEA. Interestingly, one of the pathways significantly elevated in *iKras- Yap1*$^{Amp-}$ cells was non-canonical WNT pathway[33] (Fig.4C, Supplementary Table 9), which has been recently shown to suppresses Hippo signaling and activate YAP1 in adipocytes[34]. Importantly, a moderate but significant correlation between non-canonical WNT signature and YAP1 activation signature was observed in both TCGA and ICGC dataset (Fig.4D&S5A), suggesting control of YAP1 activation by non-canonical WNT pathway in PDAC. A survey of WNT ligands identified *Wnt5a*, the prototypic non-canonical WNT ligand[35], to be exclusively overexpressed in the *iKras- Yap1*$^{Amp-}$ tumor cells at both mRNA and protein levels (Fig.4E&S5B). Moreover, *WNT5A* expression was also significantly elevated in squamous subtype compared to progenitor subtype tumors in the TCGA, while the difference in ICGC dataset does not reach statistical significance (Fig.4F&S5C). Deletion of *Wnt5a* with CRISPR in two independent *iKras- Yap1*$^{Amp-}$ tumor cell lines lead to the induction of YAP1 phosphorylation at S127, increase in cytoplasmic retention of YAP1 protein as well as downregulation of YAP1 downstream target genes (Fig.4G-I). Additionally, ectopic expression of *Wnt5a* in *Kras*^{G12D}-driven tumor cells leads to decrease in YAP1 phosphorylation (Fig.4J), further supporting the notion that

WNT5A expression drives YAP1 activation in mouse PDAC cells. We further validated these findings in human PDAC cell lines where WNT5A expression was found to be highly elevated in the YAP1-dependent PaTu8988T cells, in contrast to PaTu8988S cells, derived from same patient but with low YAP1 activation (Fig.4E). Ectopic expression of WNT5A in PaTu8988S cells reduced YAP1 phosphorylation and enhanced YAP1 nuclear localization (Fig.4J&K). On the other hand, depletion of WNT5A in PaTu8988T cells with shRNA resulted in elevated YAP1 phosphorylation (Fig.4L). Taken together, our data indicates that WNT5A overexpression can lead to YAP1 activation in PDAC cells.

WNT5A overexpression enables tumor maintenance and bypass of KRAS-dependence

At functional level, *Wnt5a* deletion in *iKras- Yap1*$^{Amp-}$ tumor cells with CRISPR significantly inhibited colony formation (Fig.5A&B). In agreement with the genetic ablation, treatment with WNT5A antagonist, BOX-5, specifically induced YAP1 phosphorylation and abolished the colony formation ability of *iKras- Yap1*$^{Amp-}$ tumor cells, but not the *Yap1*$^{Amp+}$ cells (Fig.5C-E). Moreover, *Wnt5a* deletion also significantly inhibited xenograft tumor growth in vivo, which was rescued by reconstituted WNT5A expression (Fig.5F&G). Importantly, in contrast to the predominant nuclear staining of YAP1 in the parental *iKras- Yap1*$^{Amp-}$ cells, *Wnt5a* knockout tumors exhibited significant amount of cytoplasmic YAP1 whereas WNT5A reconstitution restored YAP1 nuclear accumulation without affecting total YAP1 expression level (Fig.5H-I, S5D), implicating the diminished tumor growth to decreased YAP1 activity. Consistent with the role of YAP1 in driving squamous subtype, expression of squamous subtype genes (*Cav1* and *Pappa*) was suppressed in *Wnt5a* KO tumors whereas the expression of progenitor subtype genes (*Tff1* and *Muc13*) was induced, which was partially reversed upon WNT5A reconstitution (Fig.S5E). In addition, expression of constitutive active YAP1^{S127A} largely rescued the inhibitory effect of *Wnt5a* deletion on tumor growth (Fig.5G), thus indicating WNT5A overexpression in mouse PDAC cells

promotes tumor growth by activating YAP1. In agreement with this notion, depletion of WNT5A in human PDAC cell line, PaTu8988T cells, significantly inhibited their colony formation ability (Fig.5J).

Since YAP1 activation can maintain tumor growth upon genetic extinction of KRAS oncogene in PDAC[5 29], we next investigated if WNT5A overexpression can also serve to bypass KRAS-dependency. Indeed, ectopic expression of WNT5A in *Kras*^{G12D}-driven iKras tumor cells and KRAS-dependent PaTu8988S cells partially restored the colony formation upon KRAS depletion (Fig.6A, S6A-B). In addition, forced WNT5A expression in *Kras*^{G12D}-driven iKras tumor spheres was able to maintain cell viability upon extinction of *Kras*^{G12D} by doxycycline withdrawal whereas most control tumor cells expressing GFP underwent apoptosis (Fig.6B-D). Importantly, the survival effect of WNT5A upon *Kras*^{G12D} extinction was largely abolished upon YAP1 knockdown (Fig.6B-D), indicating that YAP1 is required for WNT5A-induced bypass of KRAS-dependence. Indeed, similar to the effect of YAP1^{S127A}, ectopic WNT5A expression in iKras tumor cells showed KRAS-independent tumor growth when injected orthotopically into nude mice, whereas GFP-expressing iKras tumor cells failed to maintain tumor growth in the absence of doxycycline (Fig. 6E-G). Importantly, WNT5A-induced KRAS-independent tumor growth is abolished in *Yap1* deleted cells (Fig. S6C-D), underlying the requirement of YAP1 for WNT5A-mediated bypass of KRAS-dependence. Notably, all WNT5A-driven tumors showed lower MAPK activity and strong nuclear YAP1 accumulation as compared to *Kras*^{G12D}-driven tumors (Fig.6H). Together, these results indicate that WNT5A overexpression can activate YAP1 and substitute for oncogenic Kras-driven tumor maintenance.

WNT5A-YAP1 axis functions in primary human PDAC

Since WNT5A is not frequently overexpressed in established human PDAC cell lines (Fig.S2G), we further validated the WNT5A-YAP1 axis in our collection of PDAC PDXs. As shown in Fig.7A-C, *WNT5A* expression is elevated in squamous subtype tumors and is significantly correlated with YAP1

signature in both PDXs and TCGA dataset, although the correlation is relatively moderate. Accordingly, WNT5A was highly expressed while YAP1 phosphorylation was relatively low in squamous subtype PATC148 and PATC153 cells, while two cell lines derived from progenitor subtype tumors, PATC102 and PATC108, exhibited elevated YAP1 phosphorylation along with absence of WNT5A expression (Fig.7D). This is in accordance with the elevated expression of YAP1 target gene CYR61 and the dependence on YAP1 oncogene in squamous subtype PDXs (Fig.3C-D, 7D).

Consistent with our findings in known human PDAC cell lines and primary mouse tumor lines, shRNA-mediated depletion of WNT5A in PDX-derived PATC148 (*Kras*^{G12D}) and PATC153 (*Kras* WT) cells caused increase in YAP1 phosphorylation, suppression of the colony formation ability and diminished tumor growth in vivo (Fig.7E-H), supporting the role of WNT5A for the tumorigenic activity. In contrast, WNT5A shRNA has minimal effect on the in vivo tumor growth of PATC108 cells. Consistent with the role of WNT5A in bypass of KRAS-dependence, knockdown of KRAS elicited less inhibition on the growth of high WNT5A expressing PATC148 (KRAS^{G12D}) cells compared to low WNT5A expressing PATC102 (KRAS^{G12D}) and PATC108 (KRAS^{G12D}) cells, with KRAS WT PATC153 cells being resistant to KRAS knockdown (Fig.7I&J). Together, our data indicates that WNT5A overexpression in squamous subtype PDACs contributes to YAP1 activation and tumor growth.

Discussion

YAP1 is activated in many cancer types and has been shown to be essential for tumor initiation and progression, including pancreatic cancer[36]. In this study, we found that PDAC development driven by *Kras*^{G12D} and *Trp53*^{R172H} in adult mice was marked by YAP1 activation, evident by its strong nuclear expression in tumor epithelium (Fig.1D). Subsequently, concurrent deletion of *Yap1* in adult pancreas completely blocked PDAC development (Fig.1E-G). Immunohistochemical staining on these tumor tissues showed marked decrease in cell proliferation index, as measured by Ki-67 staining (Fig.S1A) and high Survivin (BIRC5) expression (Fig.1H). Since, Survivin expression overlapped with YAP1 expression

in *Yap1*-WT PDAC but completely lost in *Yap1*-KO pancreas, it is likely regulated directly by YAP1 at transcription level, as shown in esophageal squamous cell carcinoma[37]. Survivin is a known anti-apoptotic protein, which is expressed only in tumor cells[38] and mostly during G2-mitotic phases of cell cycle[39]. The mostly nuclear expression of Survivin that is observed in YAP-WT tumor sections (Fig.1H) supports its predominant role in regulating cell cycle. Accordingly, higher Survivin expression was also in agreement with predominant gene signatures associated with cell cycle progression in Pa04C-YAP1^{S127A} cells (Supplementary Table 3) and higher percentage of Pa04C-YAP1^{S127A} cells in G2/M phase by cell cycle analysis (data not shown).

We provided evidence that YAP1 is highly activated in squamous subtype PDACs and required for their tumorigenic function. Moreover, we show that enforced YAP1 activation was able to convert the gene expression signature of PDAC cells from progenitor to squamous subtype, further indicating that YAP1 may function as a major driver for squamous subtype tumors and thus could be a potential therapeutic target in this highly malignant subgroup. The squamous subtype PDAC was characterized by high expression of mesenchyme-associated genes with PDAC cell lines enriched within squamous subtype exhibiting features of EMT[8 10 40]. Moreover, the KRAS-independent mouse PDAC tumors, which were YAP1-dependent and reminiscent of squamous subtype tumors, were also highly enriched with EMT signature (data not shown), thus implicating YAP1 in promoting aggressive behavior of squamous subtype PDAC through EMT. In fact, YAP1 has been shown to be a potent inducer of EMT in tumor cells[29]. Recently, ZEB1, a key EMT transcription factor, was shown to be critical for PDAC metastasis[41], and required for the transcription of YAP1 downstream targets by direct bind with YAP1[42]. Further studies are warranted to verify whether EMT is indeed required for YAP1-driven aggressive behavior, such as metastasis in PDAC.

Despite the emerging role of *YAP1* as a major oncogene in multiple cancer types, genetic alterations of *YAP1* gene or its upstream Hippo pathway are relatively uncommon[43 44]. YAP1 amplification or mutations in *NF2*, an upstream negative regulator of YAP1 activity, has been reported in around 1% of human PDAC[8 45]. Therefore, the activation of YAP1 in advanced human PDAC is likely due to non-genetic factors regulating inhibitory upstream Hippo kinases. Our data showing constitutive nuclear localization of YAP1 protein in YAP1-dependent tumor cells, indicates that the suppression of Hippo signaling is the major mechanism for YAP1 activation in PDAC. While investigating upstream regulator of YAP1 activation, we found evidence that WNT5A overexpression leads to YAP1 activation and bypass of KRAS-dependency in KRAS-independent mouse PDAC cells and a subset of human squamous subtype PDACs. WNT5A is a prototypic non-canonical WNT ligand[35] and has been implicated in the pathogenesis of PDAC[46 47]. It has been recently shown that WNT5A-mediated non-canonical WNT pathway suppresses Hippo signaling and activates YAP1 through G protein-dependent activation of Rho GTPases[34]. WNT5A can also engage multiple additional downstream signaling pathways, including SRC and PKC, which have been shown to activate YAP1 through direct phosphorylation or indirectly through the regulation of Rho GTPases and LATS activity[48-53]. Interestingly, it was recently reported that non-canonical WNT and FZD8 mediated calcium signaling counteracts the tumorigenic activity of oncogenic KRAS[54]. On the other hand, FZD1 was shown to be important for WNT5A-mediated YAP1 activation[34]. It's possible that the engagement of specific receptors by WNT5A determines its signaling and biological output in PDAC. It remains to be further validated if any particular one or all of these mechanisms are responsible for WNT5A-mediated YAP1 activation in PDAC. In addition, it's likely additional non-canonical WNT ligands are also involved in YAP1 activation in PDAC. Among them, WNT7B expression is also elevated in squamous subtype PDAC and is correlated with YAP1 activation signature (Data not shown). It remains

to be determined whether the additional non-canonical WNT ligands also contribute to YAP1 activation in PDAC.

While our data indicates WNT5A overexpression in tumor cells functions in cell-autonomous manner to activate YAP1 oncoprotein, tumor cells may also get active WNT5A signaling through paracrine mechanisms. Interestingly, WNT5A has been shown to be highly expressed in PDAC stroma fibroblast[55 56], and our preliminary data implicates that stroma WNT5A level is significantly correlated with tumor cell YAP1 level in human PDAC (data not shown). Therefore, stromal WNT5A could possibly contributes to YAP1 activation in tumor cells, given that the exuberant desmoplastic stroma is a defining characteristic of PDAC[2]. In this scenario, the tumor-stroma interaction will thus play an instrumental role in orchestrating the heterogeneous YAP1 activation in bulk tumor which may, in turn, define the molecular heterogeneity and diverse biological phenotypes of PDAC.

Taken together, with agents targeting the Hippo-YAP pathway under development[43], our study showing the critical role of WNT5A-mediated YAP1 activation in a subset of pancreatic tumors of squamous subtype provides viable therapeutic targets for this most malignant form of human PDAC.

Acknowledgements

We thank the laboratory of Dr. Ben Stanger for sharing mouse PDAC cell lines, PD3077. We would like to thank the Institute for Applied Cancer Science (IACS), the Flow Cytometry and Cellular Imaging Core, the Department of Veterinary Medicine at The University of Texas MD Anderson Cancer Center (Cancer Center Support Grant, CA016672). We thank Dr. Ronald DePinho, Dr. Alan Wang, Dr. Mien-Chie Hung, Dr. Guocan Wang, Dr. Baoli Hu, Dr. Xin Zhou and Dr. Jihye Paik for helpful discussions and critical reviews. The research was supported by the Pancreatic Cancer Action Network-AACR Career Development Award to H.Y.; the Pancreatic Cancer Action Network-AACR Pathway to Leadership

Award to W.Y.; Seed Grant from Hirshberg foundation for pancreatic cancer research to H.Y. and W.Y., P01 Grant (P01CA117969 12, NIH) to H.W., J.B.F., M.K., G.F.D., A.M. and H.Y.

Competing Interests

The authors declare no competing interests.

Reference:

1. Rahib L, Smith BD, Aizenberg R, et al. Projecting cancer incidence and deaths to 2030: the unexpected burden of thyroid, liver, and pancreas cancers in the United States. *Cancer Res* 2014;74(11):2913-21. doi: 10.1158/0008-5472.CAN-14-0155

2. Ying H, Dey P, Yao W, et al. Genetics and biology of pancreatic ductal adenocarcinoma. *Genes Dev* 2016;30(4):355-85. doi: 10.1101/gad.275776.115

3. Collins MA, Bednar F, Zhang Y, et al. Oncogenic Kras is required for both the initiation and maintenance of pancreatic cancer in mice. *J Clin Invest* 2012;122(2):639-53. doi: 10.1172/JCI59227 [published Online First: 2012/01/11]

4. Ying H, Kimmelman AC, Lyssiotis CA, et al. Oncogenic Kras maintains pancreatic tumors through regulation of anabolic glucose metabolism. *Cell* 2012;149(3):656-70. doi: 10.1016/j.cell.2012.01.058 [published Online First: 2012/05/01]

5. Kapoor A, Yao W, Ying H, et al. Yap1 activation enables bypass of oncogenic Kras addiction in pancreatic cancer. *Cell* 2014;158(1):185-97. doi: 10.1016/j.cell.2014.06.003 [published Online First: 2014/06/24]

6. Muzumdar MD, Chen PY, Dorans KJ, et al. Survival of pancreatic cancer cells lacking KRAS function. *Nat Commun* 2017;8(1):1090. doi: 10.1038/s41467-017-00942-5

7. Viale A, Pettazzoni P, Lyssiotis CA, et al. Oncogene ablation-resistant pancreatic cancer cells depend on mitochondrial function. *Nature* 2014;514(7524):628-32. doi: 10.1038/nature13611 [published Online First: 2014/08/15]

8. Bailey P, Chang DK, Nones K, et al. Genomic analyses identify molecular subtypes of pancreatic cancer. *Nature* 2016;531(7592):47-52. doi: 10.1038/nature16965

9. Cancer Genome Atlas Research Network. Electronic address aadhe, Cancer Genome Atlas Research N. Integrated Genomic Characterization of Pancreatic Ductal Adenocarcinoma. *Cancer Cell* 2017;32(2):185-203 e13. doi: 10.1016/j.ccell.2017.07.007

10. Collisson EA, Sadanandam A, Olson P, et al. Subtypes of pancreatic ductal adenocarcinoma and their differing responses to therapy. *Nat Med* 2011;17(4):500-3. doi: 10.1038/nm.2344 [published Online First: 2011/04/05]

11. Moffitt RA, Marayati R, Flate EL, et al. Virtual microdissection identifies distinct tumor- and stroma-specific subtypes of pancreatic ductal adenocarcinoma. *Nat Genet* 2015;47(10):1168-78. doi: 10.1038/ng.3398

12. Meng Z, Moroishi T, Guan KL. Mechanisms of Hippo pathway regulation. *Genes Dev* 2016;30(1):1-17. doi: 10.1101/gad.274027.115

13. Zhao B, Wei X, Li W, et al. Inactivation of YAP oncoprotein by the Hippo pathway is involved in cell contact inhibition and tissue growth control. *Genes Dev* 2007;21(21):2747-61. doi: 10.1101/gad.1602907 [published Online First: 2007/11/03]

14. Gao T, Zhou D, Yang C, et al. Hippo signaling regulates differentiation and maintenance in the exocrine pancreas. *Gastroenterology* 2013;144(7):1543-53, 53 e1. doi: 10.1053/j.gastro.2013.02.037 [published Online First: 2013/03/05]

15. Kopp JL, von Figura G, Mayes E, et al. Identification of Sox9-dependent acinar-to-ductal reprogramming as the principal mechanism for initiation of pancreatic ductal adenocarcinoma. *Cancer Cell* 2012;22(6):737-50. doi: 10.1016/j.ccr.2012.10.025

16. Gruber R, Panayiotou R, Nye E, et al. YAP1 and TAZ Control Pancreatic Cancer Initiation in Mice by Direct Upregulation of JAK-STAT3 Signaling. *Gastroenterology* 2016 doi: 10.1053/j.gastro.2016.05.006

17. Zhang W, Nandakumar N, Shi Y, et al. Downstream of mutant KRAS, the transcription regulator YAP is essential for neoplastic progression to pancreatic ductal adenocarcinoma. *Sci Signal* 2014;7(324):ra42. doi: 10.1126/scisignal.2005049

18. Salcedo Allende MT, Zeron-Medina J, Hernandez J, et al. Overexpression of Yes Associated Protein 1, an Independent Prognostic Marker in Patients With Pancreatic Ductal Adenocarcinoma, Correlated With Liver Metastasis and Poor Prognosis. *Pancreas* 2017;46(7):913-20. doi: 10.1097/MPA.0000000000000867 [published Online First: 2017/07/12]

19. Wei H, Xu Z, Liu F, et al. Hypoxia induces oncogene yes-associated protein 1 nuclear translocation to promote pancreatic ductal adenocarcinoma invasion via epithelial-mesenchymal transition. *Tumour Biol* 2017;39(5):1010428317691684. doi: 10.1177/1010428317691684 [published Online First: 2017/05/06]

20. Morvaridi S, Dhall D, Greene MI, et al. Role of YAP and TAZ in pancreatic ductal adenocarcinoma and in stellate cells associated with cancer and chronic pancreatitis. *Sci Rep* 2015;5:16759. doi: 10.1038/srep16759

21. Habbe N, Shi G, Meguid RA, et al. Spontaneous induction of murine pancreatic intraepithelial neoplasia (mPanIN) by acinar cell targeting of oncogenic Kras in adult mice. *Proc Natl Acad Sci U S A* 2008;105(48):18913-8. doi: 10.1073/pnas.0810097105

22. Cai J, Zhang N, Zheng Y, et al. The Hippo signaling pathway restricts the oncogenic potential of an intestinal regeneration program. *Genes Dev* 2010;24(21):2383-8. doi: 10.1101/gad.1978810

23. Jones S, Zhang X, Parsons DW, et al. Core signaling pathways in human pancreatic cancers revealed by global genomic analyses. *Science* 2008;321(5897):1801-6. doi: 10.1126/science.1164368 [published Online First: 2008/09/06]

24. Aguirre AJ, Bardeesy N, Sinha M, et al. Activated Kras and Ink4a/Arf deficiency cooperate to produce metastatic pancreatic ductal adenocarcinoma. *Genes Dev* 2003;17(24):3112-26.

25. Cordenonsi M, Zanconato F, Azzolin L, et al. The Hippo transducer TAZ confers cancer stem cell-related traits on breast cancer cells. *Cell* 2011;147(4):759-72. doi: 10.1016/j.cell.2011.09.048

26. Elsasser HP, Lehr U, Agricola B, et al. Establishment and characterisation of two cell lines with different grade of differentiation derived from one primary human pancreatic adenocarcinoma. *Virchows Arch B Cell Pathol Incl Mol Pathol* 1992;61(5):295-306.

27. Kim MH, Kim J, Hong H, et al. Actin remodeling confers BRAF inhibitor resistance to melanoma cells through YAP/TAZ activation. *EMBO J* 2016;35(5):462-78. doi: 10.15252/embj.201592081

28. Lin L, Sabnis AJ, Chan E, et al. The Hippo effector YAP promotes resistance to RAF- and MEK-targeted cancer therapies. *Nat Genet* 2015;47(3):250-6. doi: 10.1038/ng.3218

29. Shao DD, Xue W, Krall EB, et al. KRAS and YAP1 converge to regulate EMT and tumor survival. *Cell* 2014;158(1):171-84. doi: 10.1016/j.cell.2014.06.004

30. Sweet-Cordero A, Mukherjee S, Subramanian A, et al. An oncogenic KRAS2 expression signature identified by cross-species gene-expression analysis. *Nat Genet* 2005;37(1):48-55. doi: 10.1038/ng1490 [published Online First: 2004/12/21]

31. Barbie DA, Tamayo P, Boehm JS, et al. Systematic RNA interference reveals that oncogenic KRAS-driven cancers require TBK1. *Nature* 2009;462(7269):108-12.

32. Aiello NM, Maddipati R, Norgard RJ, et al. EMT Subtype Influences Epithelial Plasticity and Mode of Cell Migration. *Developmental cell* 2018;45(6):681-95 e4. doi: 10.1016/j.devcel.2018.05.027 [published Online First: 2018/06/20]

33. Schaefer CF, Anthony K, Krupa S, et al. PID: the Pathway Interaction Database. *Nucleic Acids Res* 2009;37(Database issue):D674-9. doi: 10.1093/nar/gkn653

34. Park HW, Kim YC, Yu B, et al. Alternative Wnt Signaling Activates YAP/TAZ. *Cell* 2015;162(4):780-94. doi: 10.1016/j.cell.2015.07.013

35. van Amerongen R. Alternative Wnt pathways and receptors. *Cold Spring Harb Perspect Biol* 2012;4(10) doi: 10.1101/cshperspect.a007914

36. Zanconato F, Cordenonsi M, Piccolo S. YAP/TAZ at the Roots of Cancer. *Cancer Cell* 2016;29(6):783-803. doi: 10.1016/j.ccell.2016.05.005

37. Muramatsu T, Imoto I, Matsui T, et al. YAP is a candidate oncogene for esophageal squamous cell carcinoma. *Carcinogenesis* 2011;32(3):389-98. doi: 10.1093/carcin/bgq254

38. Ambrosini G, Adida C, Altieri DC. A novel anti-apoptosis gene, survivin, expressed in cancer and lymphoma. *Nature medicine* 1997;3(8):917-21.

39. Caldas H, Jiang Y, Holloway MP, et al. Survivin splice variants regulate the balance between proliferation and cell death. *Oncogene* 2005;24(12):1994-2007. doi: 10.1038/sj.onc.1208350

40. Singh A, Settleman J. Oncogenic K-ras "addiction" and synthetic lethality. *Cell Cycle* 2009;8(17):2676-7. doi: 9336 [pii] [published Online First: 2009/08/20]

41. Krebs AM, Mitschke J, Lasierra Losada M, et al. The EMT-activator Zeb1 is a key factor for cell plasticity and promotes metastasis in pancreatic cancer. *Nat Cell Biol* 2017;19(5):518-29. doi: 10.1038/ncb3513

42. Lehmann W, Mossmann D, Kleemann J, et al. ZEB1 turns into a transcriptional activator by interacting with YAP1 in aggressive cancer types. *Nat Commun* 2016;7:10498. doi: 10.1038/ncomms10498

43. Harvey KF, Zhang X, Thomas DM. The Hippo pathway and human cancer. *Nat Rev Cancer* 2013;13(4):246-57. doi: 10.1038/nrc3458 [published Online First: 2013/03/08]

44. Yu FX, Zhao B, Guan KL. Hippo Pathway in Organ Size Control, Tissue Homeostasis, and Cancer. *Cell* 2015;163(4):811-28. doi: 10.1016/j.cell.2015.10.044

45. Mueller S, Engleitner T, Maresch R, et al. Evolutionary routes and KRAS dosage define pancreatic cancer phenotypes. *Nature* 2018;554(7690):62-68. doi: 10.1038/nature25459

46. Schwartz AL, Malgor R, Dickerson E, et al. Phenylmethimazole decreases Toll-like receptor 3 and noncanonical Wnt5a expression in pancreatic cancer and melanoma together with tumor cell

growth and migration. *Clin Cancer Res* 2009;15(12):4114-22. doi: 10.1158/1078-0432.CCR-09-0005

47. Ripka S, Konig A, Buchholz M, et al. WNT5A--target of CUTL1 and potent modulator of tumor cell migration and invasion in pancreatic cancer. *Carcinogenesis* 2007;28(6):1178-87. doi: 10.1093/carcin/bgl255

48. Gong R, Hong AW, Plouffe SW, et al. Opposing roles of conventional and novel PKC isoforms in Hippo-YAP pathway regulation. *Cell Res* 2015;25(8):985-8. doi: 10.1038/cr.2015.88

49. Grzeschik NA, Parsons LM, Allott ML, et al. Lgl, aPKC, and Crumbs regulate the Salvador/Warts/Hippo pathway through two distinct mechanisms. *Current biology : CB* 2010;20(7):573-81. doi: 10.1016/j.cub.2010.01.055

50. Kim NG, Gumbiner BM. Adhesion to fibronectin regulates Hippo signaling via the FAK-Src-PI3K pathway. *J Cell Biol* 2015;210(3):503-15. doi: 10.1083/jcb.201501025

51. Li P, Silvis MR, Honaker Y, et al. alphaE-catenin inhibits a Src-YAP1 oncogenic module that couples tyrosine kinases and the effector of Hippo signaling pathway. *Genes Dev* 2016;30(7):798-811. doi: 10.1101/gad.274951.115

52. Sudol M. Yes-associated protein (YAP65) is a proline-rich phosphoprotein that binds to the SH3 domain of the Yes proto-oncogene product. *Oncogene* 1994;9(8):2145-52.

53. Zaidi SK, Sullivan AJ, Medina R, et al. Tyrosine phosphorylation controls Runx2-mediated subnuclear targeting of YAP to repress transcription. *EMBO J* 2004;23(4):790-9. doi: 10.1038/sj.emboj.7600073

54. Wang MT, Holderfield M, Galeas J, et al. K-Ras Promotes Tumorigenicity through Suppression of Non-canonical Wnt Signaling. *Cell* 2015;163(5):1237-51. doi: 10.1016/j.cell.2015.10.041

55. Pilarsky C, Ammerpohl O, Sipos B, et al. Activation of Wnt signalling in stroma from pancreatic cancer identified by gene expression profiling. *J Cell Mol Med* 2008;12(6B):2823-35. doi: 10.1111/j.1582-4934.2008.00289.x

56. Seino T, Kawasaki S, Shimokawa M, et al. Human Pancreatic Tumor Organoids Reveal Loss of Stem Cell Niche Factor Dependence during Disease Progression. *Cell Stem Cell* 2018 doi: 10.1016/j.stem.2017.12.009

Figure Legends

Figure 1. YAP1 is essential for PDAC development.

(A) Representative images of YAP1 TMA showing tumor adjacent normal pancreatic tissue or tumor samples with low/high YAP1 level. Scale bar: 200 μm. (B-C) Kaplan-Meier curves for overall survival in PDAC patients from MDA (B) or JHU (C) stratified by YAP1 expression. (D) *Yap1* wild-type (WT) or knockout (KO) MKP mice driven by tamoxifen-inducible *Mist1-Cre*^{ERT2}. Pancreata were collected at indicated time points and YAP1 staining shows YAP1 activation in PDAC tumors of MKP mice. Scale bar: 50μm. (E-F) Gross images of pancreata (E) and H&E staining (F) shows block of tumor development in *Yap1*-KO mice. Scale bar: 100μm. (G) Kaplan-Meier overall survival analysis for mice of indicated genotypes shows complete survival of *Yap1*-KO mice in contrast with median survival of 103 days in *Yap1*-WT mice. p value for survival analysis was calculated with log rank test. (H) Pancreata from *Yap1* wild-type (WT) or knockout (KO) MKP mice were collected at indicated time points and stained for Survivin. For each time point (age group), at least 4 mice per genotype were analyzed. Scale bar: 100μm.

Figure 2. YAP1 enhances the malignant phenotypes of PDAC and is activated in squamous subtype.

(A) Ectopic expression of YAP1^{S127A} in PaTu8988S and Pa04C cells promotes anchorage-independent growth in soft agar (quantification from triplicates shown in bottom panel) and cell invasion in a Boyden chamber assay (B) (Quantification of triplicates is shown in (C)). (D) Orthotopic xenograft tumors from Pa04C-Vector or -YAP1^{S127A} cells were established in immunocompromised mice (top). Red arrows indicate primary tumors and white arrows indicate metastatic tumors grown on peritoneum, lymph node and liver. Metastasis rate and involved organs are summarized in bottom panel. (E) H&E staining of orthotopic primary and metastatic tumors generated from Pa04C cells shows large necrotic areas in Pa04C-Vector tumors only while confirming metastases of Pa04C-YAP1^{S127A} (mYAP) cells in liver (Liv), lung (Lu), diaphragm (Dia) and lymph node (LN). Scale bar: 100μm. (F) YAP1 signature score among

human PDAC subtypes. Heatmap of the YAP1 signature gene expression is shown in (G). ADEX (A): aberrantly differentiated endocrine exocrine subtype; Immu (I): immunogenic subtype; Pro (P): progenitor subtype; SQ (S): squamous subtype. (H) Correlation between squamous subtype signature and YAP1 signature in PDAC TCGA and ICGC dataset. (I) Kaplan-Meier curves for overall survival in all PDAC patients or non-squamous subtype PDAC patients (J) from ICGC dataset stratified by YAP1 activation signature score. (K) YAP1 signature score in squamous (SQ) or progenitor (Pro) subtype human PDAC cell lines or PDXs (L). Error bars from all panels indicate ±SD. *: $p<0.05$; **: $p<0.01$. p value for survival analysis was calculated with log rank test.

Figure 3. YAP1 is essential for the maintenance of squamous subtype PDACs

(A) Representative images of the colony formation assay in human PDAC cell lines infected with YAP1 shRNAs or non-targeting shRNA (shCtr). The YAP1 knockdown efficiency was detected by Western blot. Quantification from triplicates is shown in (B) and is presented as relative colony numbers upon normalization to shCtr group. (C) Representative images of the colony formation assay in PDX cells infected with YAP1 shRNAs or non-targeting shRNA (shCtr). Quantification of from triplicates is shown in (D). (E) Representative images of the cell growth assay in human PDAC cell lines infected with KRAS shRNAs or non-targeting shRNA (shCtr). Quantification from triplicates is shown in (F) and is presented as relative growth upon normalization to shCtr group. (G) KRAS-independence signature score among human PDAC subtypes. SQ: squamous subtype; Pro: progenitor subtype; ADEX: aberrantly differentiated endocrine exocrine subtype; Immu: immunogenic subtype. (H) YAP1 signature score among mouse PDAC tumors with indicated genotypes. (I) Representative images of the colony formation assay in mouse PDAC cells infected with Yap1 shRNAs or non-targeting shRNA (shCtr). Quantification of colony formation from triplicates is shown in (J). Error bars from all panels indicate ±SD. *: $p<0.05$; **: $p<0.01$.

Figure 4. YAP1 activation in PDAC is mediated by WNT5A overexpression

(A) Human pancreatic cancer cell lines of progenitor or squamous subtype or mouse PDAC cells of indicated genotypes (B) were subjected to immunofluorescence staining with anti-YAP1 (red) and DAPI (blue). (C) Non-canonical (NC) WNT pathway enrichment score in iKras- mouse PDAC tumors without (Amp-) or with (Amp+) *Yap1* amplification. (D) Correlation between non-canonical WNT signature and YAP1 signature in PDAC TCGA dataset. (E) Western blots for WNT5A in mouse PDAC cells of indicated genotypes and human PDAC cell lines. (F) *WNT5A* expression in squamous (SQ) or progenitor (Pro) subtype human PDACs in TCGA dataset. (G) Western blot analysis for WNT5A, YAP1 and phospho-YAP1 (S127) in two independent *iKras-Yap1*$^{Amp-}$ cells with CRISPR-mediated *Wnt5a* deletion. Two independent *Wnt5a* knockout (KO) clones were included and clone without *Wnt5a* deletion was used as control (Ctr). (H) E-4 (*iKras-Yap1*$^{Amp-}$)-*Wnt5a* KO cells were subjected to immunofluorescence staining with anti-YAP1 (red) and DAPI (blue). (I) Relative mRNA levels of YAP1 downstream targets in E-4 (*iKras-Yap1*$^{Amp-}$)-*Wnt5a* KO cells. (J) Western blot analysis for WNT5A, YAP1 and phospho-YAP1 (S127) in mouse iKras PDAC cells (AK192) or human PaTu8988S cells expressing GFP or WNT5A (Top). The quantification of phosphor-YAP1/total YAP1 signals is shown in the bottom panel. (K) PaTu8988S cells expressing GFP or WNT5A were subjected to immunofluorescence staining with anti-YAP1 (red) and DAPI (blue). (L) Western blot analysis for WNT5A, YAP1 and phospho-YAP1 (S127) in PaTu8988T cells infected with WNT5A shRNAs or non-targeting shRNA (shCtr). Error bars from all panels indicate ±SD. *: $p<0.05$; **: $p<0.01$. Scale bar: 20 μm.

Figure 5. WNT5A overexpression is required for tumorigenic activity

(A) Representative images of the colony formation assay for *iKras-Yap1*$^{Amp-}$-Wnt5a KO cells. Clones without *Wnt5a* deletion was used as control (Ctr). Quantification from triplicates is shown in (B) and is presented as relative colony numbers upon normalization to shCtr group. (C) Western blot analysis for YAP1 and phospho-YAP1 (S127) in mouse PDAC cells treated with DMSO, 50 or 100μM of BOX-5.

(D) Representative images of the colony formation assay in mouse PDAC cells of indicated genotypes treated with vehicle (DMSO) or WNT5A antagonist, BOX-5 (100μM). Quantification from triplicates is shown in (E) and is presented as relative colony numbers upon normalization to DMSO group. (F) Two independent clones of E-6 (*iKras- Yap1*$^{Amp-}$)-*Wnt5a* KO cells and control cells without *Wnt5a* deletion (CTR) were subcutaneously injected into nude mice. Tumor volumes were measured on the indicated dates post-injection. Results are presented as the means±SEM. (n=5). (G) E-4 (*iKras- Yap1*$^{Amp-}$)-*Wnt5a* KO cells were infected with GFP, WNT5A or YAP1^{S127A} and were subcutaneously injected into nude mice. Cells without *Wnt5a* deletion were used as control (CTR). Tumor volumes were measured 30 days post-injection. Results are presented as the means±SEM. (n=5). (H) Subcutaneous xenograft tumors from (G) were stained for YAP1, Scale bar: 100 μm. Percentage of cells with nuclear/cytoplasmic/double staining of YAP1 is shown in (I). Error bars represent SD (n=10 fields, 250 celss/field), (J) Representative images of the colony formation assay for PaTu8988T cells infected with WNT5A shRNAs or non-targeting shRNA (shCtr) (top). Quantification from triplicates is shown in the bottom panel. Error bars from all panels indicate ±SD. *: $p<0.05$; **: $p<0.01$.

Figure 6. WNT5A overexpression leads to the bypass of KRAS-dependency

(A) Cell growth assay for PaTu8988S-GFP or –WNT5A cells infected with KRAS shRNAs or non-targeting control shRNA. Quantification from triplicates is presented as relative cell growth upon normalization to control group. Error bars indicate ±SD of triplicates, **: $p<0.01$. (B) Western blot analysis for WNT5A and YAP1 in AK192 (*iKras+*) cells expressing GFP or WNT5A upon knockdown of YAP1 with shRNA. (C) Mouse AK192-GFP or AK192-WNT5A cells infected with non-targeting shRNA (shCtr) or YAP1 shRNA (shYap1) were grown as 3D tumor spheres in the presence or absence of doxycycline for four days. Cellular apoptosis was measured with annexin V staining. Representative images show the FACS analysis of annexin V and 7AAD staining. Numbers represent the percentage of

early apoptosis (Annexin V^+ $7AAD^-$) and late apoptosis (Annexin V^+ $7AAD^+$) populations. (D) Quantification of total apoptotic cell from (C). Doxycycline withdrawal leads to dramatic apoptosis of AK192-GFP tumor sphere. Such apoptosis induced by doxycycline withdrawal was significantly inhibited in WNT5A-expressing cells, which was partially reversed upon YAP1 knockdown. Error bars indicate SD of replicates. *: $p<0.05$; **: $p<0.01$. (E) Schematic workflow for the in vivo Kras bypass experiment. (F) AK192 cells expressing luciferase were infected with lentivirus expressing GFP, WNT5A or $YAP1^{S127A}$ and orthotopically injected into nude mice pancreas in the presence of doxycycline. Animals were withdrawn from doxycycline four days later and tumor growth was visualized by bioluminescent imaging at 8 weeks. (G) Kaplan-Meier overall survival analysis for nude mice (n=5/group) orthotopically transplanted with the cells described in (F). (H) Orthotopic xenograft tumors generated with AK192-GFP cells (on doxycycline) or AK192-WNT5A cells (off doxycycline) were stained for WNT5A, YAP1 and phospho-ERK. Scale bar: 100 μm.

Figure 7. WNT5A-YAP1 axis is active in primary human PDAC and required for tumor maintenance

(A) *WNT5A* expression in squamous (SQ) or progenitor (Pro) subtype PDXs. (B) Correlation between *WNT5A* expression level and YAP1 activation signature in PDXs. (C) Correlation between *WNT5A* expression and YAP1 signature in PDAC TCGA dataset. (D) Western blot analysis for WNT5A, YAP1, phospho-YAP1 (S127) and CYR61 in PDX cell lines of squamous or progenitor subtype. (E) Western blot analysis for WNT5A, YAP1 and phospho-YAP1 (S127) in squamous subtype PDX cell lines infected with WNT5A shRNAs or non-targeting shRNA (shCtr). (F) Representative images of the colony formation assay for squamous subtype PDX cell lines infected with WNT5A shRNAs or non-targeting shRNA (shCtr). Quantification from triplicates is shown in (G). (H) PATC108 and PATC148 cells infected with WNT5A shRNAs or non-targeting shRNA (shCtr) were subcutaneously injected into nude

mice. Tumor volumes were measured on the indicated dates post-injection and relative tumor growth normalized to day 14 was presented. Results are presented as the means±SEM. (n=5). (I) Western blot analysis for KRAS, phosphor-MEK1/2 and MEK1/2 in PDX cell lines infected with KRAS shRNAs or non-targeting shRNA (shCtr). (J) Cell growth assay for PDX cell lines infected with KRAS shRNAs or non-targeting shRNA (shCtr). Quantification from triplicates is presented as relative cell growth upon normalization to shCtr group. Error bars from all panels indicate ±SD. *: $p<0.05$; **: $p<0.01$.

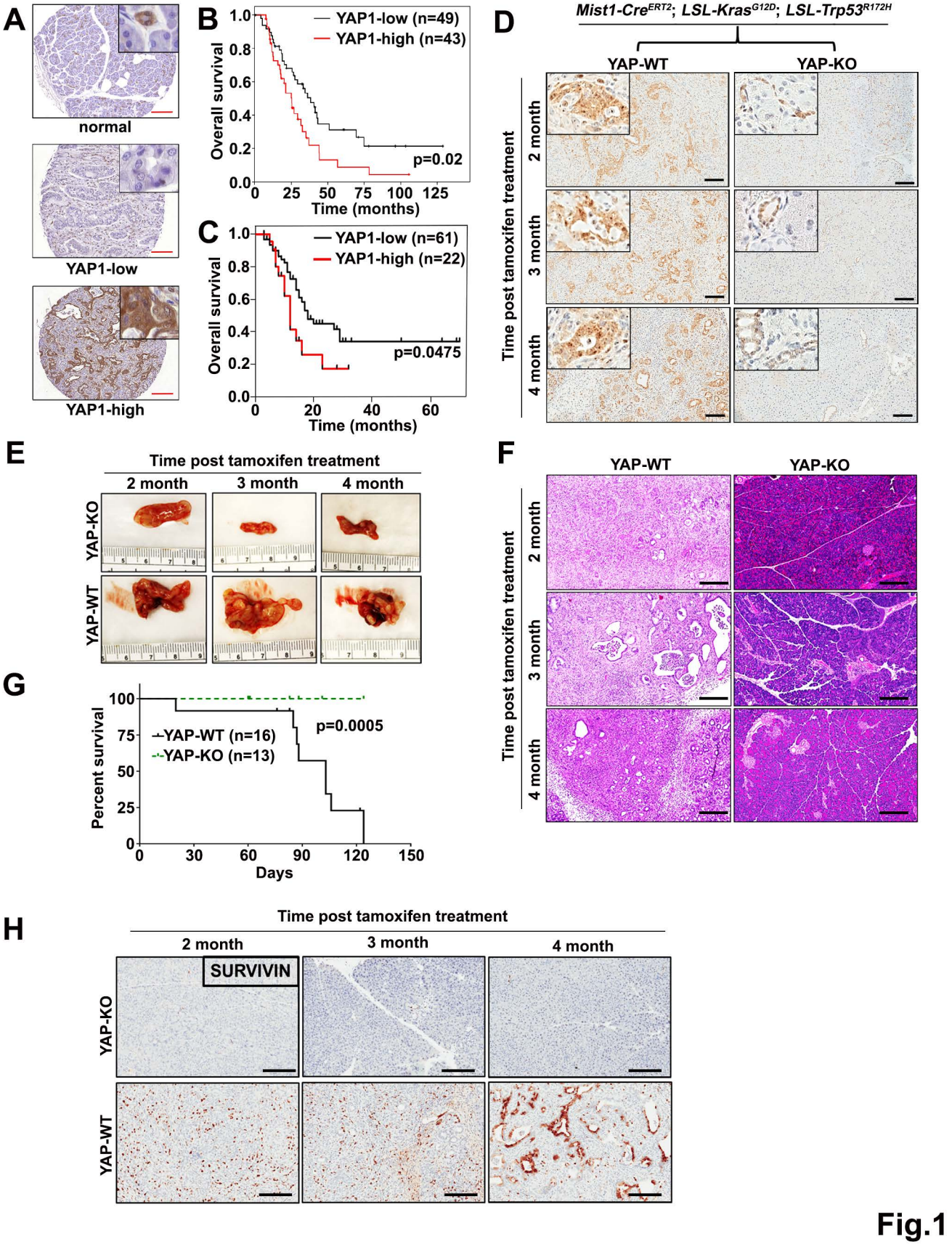
A
normal
YAP1-low
YAP1-high
B
YAP1-low (n=49)
YAP1-high (n=43)
Overall survival
p=0.02
Time (months)
C
YAP1-low (n=61)
YAP1-high (n=22)
Overall survival
p=0.0475
Time (months)
D
Mist1-CreERT2; LSL-KrasG12D; LSL-Trp53R172H
YAP-WT
YAP-KO
Time post tamoxifen treatment
2 month
3 month
4 month
E
Time post tamoxifen treatment
2 month
3 month
4 month
YAP-KO
YAP-WT
F
YAP-WT
YAP-KO
Time post tamoxifen treatment
2 month
3 month
4 month
G
Percent survival
YAP-WT (n=16)
YAP-KO (n=13)
p=0.0005
Days
H
Time post tamoxifen treatment
2 month
3 month
4 month
SURVIVIN
YAP-KO
YAP-WT

Fig.1

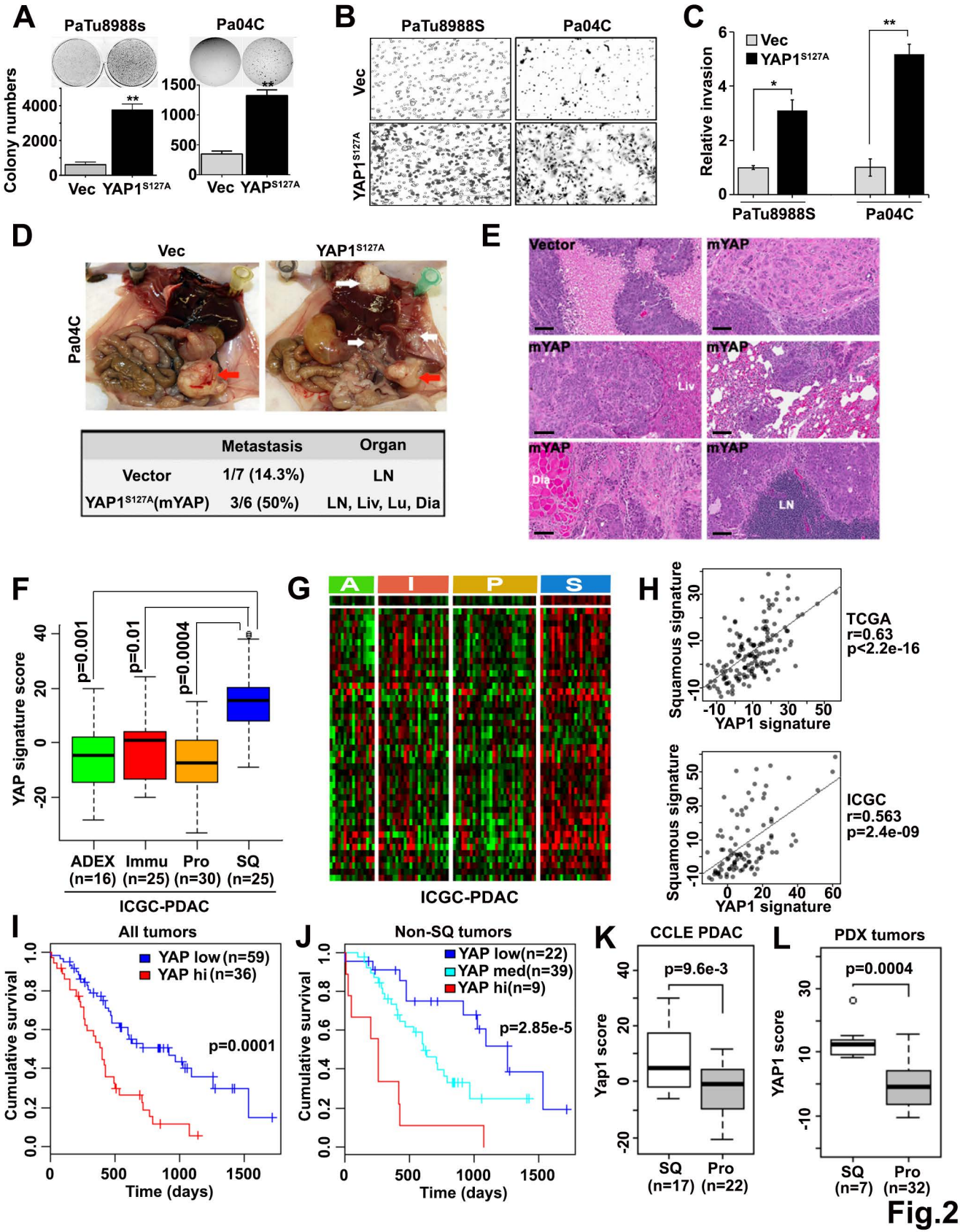
A
PaTu8988s
Pa04C
Colony numbers
Vec
YAP1S127A
YAP S127A
B
PaTu8988S
Pa04C
Vec
YAP1S127A
C
Vec
YAP1S127A
Relative invasion
PaTu8988S
Pa04C
D
Vec
YAP1S127A
Pa04C
Metastasis
Organ
Vector
1/7 (14.3%)
LN
YAP1S127A(mYAP)
3/6 (50%)
LN, Liv, Lu, Dia
E
Vector
mYAP
Liv
Lu
Dia
LN
F
YAP signature score
p=0.001
p=0.01
p=0.0004
ADEX (n=16)
Immu (n=25)
Pro (n=30)
SQ (n=25)
ICGC-PDAC
G
A
I
P
S
ICGC-PDAC
H
Squamous signature
YAP1 signature
TCGA
r=0.63
p<2.2e-16
ICGC
r=0.563
p=2.4e-09
I
All tumors
YAP low (n=59)
YAP hi (n=36)
p=0.0001
Cumulative survival
Time (days)
J
Non-SQ tumors
YAP low(n=22)
YAP med(n=39)
YAP hi(n=9)
p=2.85e-5
Cumulative survival
Time (days)
K
CCLE PDAC
p=9.6e-3
Yap1 score
SQ (n=17)
Pro (n=22)
L
PDX tumors
p=0.0004
YAP1 score
SQ (n=7)
Pro (n=32)

Fig.2

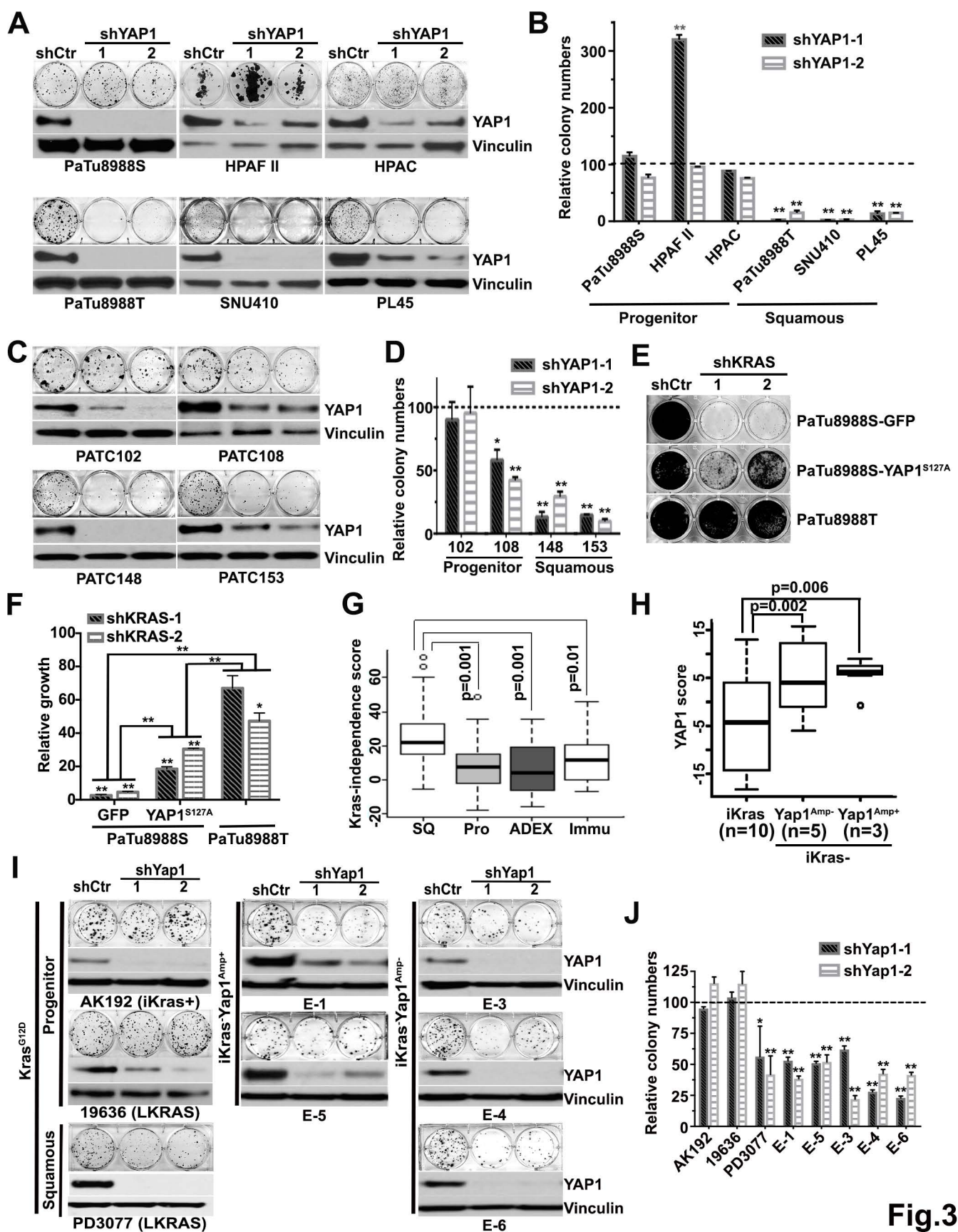
A
shYAP1
shCtr
1
2
YAP1
Vinculin
PaTu8988S
HPAF II
HPAC
PaTu8988T
SNU410
PL45
B
shYAP1-1
shYAP1-2
Relative colony numbers
Progenitor
Squamous
C
PATC102
PATC108
PATC148
PATC153
D
E
shKRAS
PaTu8988S-GFP
PaTu8988S-YAP1S127A
PaTu8988T
F
shKRAS-1
shKRAS-2
Relative growth
GFP
YAP1S127A
G
Kras-independence score
SQ
Pro
ADEX
Immu
p=0.001
p=0.001
p=0.01
H
p=0.006
p=0.002
YAP1 score
iKras (n=10)
Yap1Amp- (n=5)
Yap1Amp+ (n=3)
iKras-
I
shYap1
KrasG12D
Progenitor
Squamous
AK192 (iKras+)
19636 (LKRAS)
PD3077 (LKRAS)
iKras-Yap1Amp+
iKras-Yap1Amp-
E-1
E-5
E-3
E-4
E-6
J
shYap1-1
shYap1-2
AK192
19636
PD3077
E-1
E-5
E-3
E-4
E-6

Fig.3

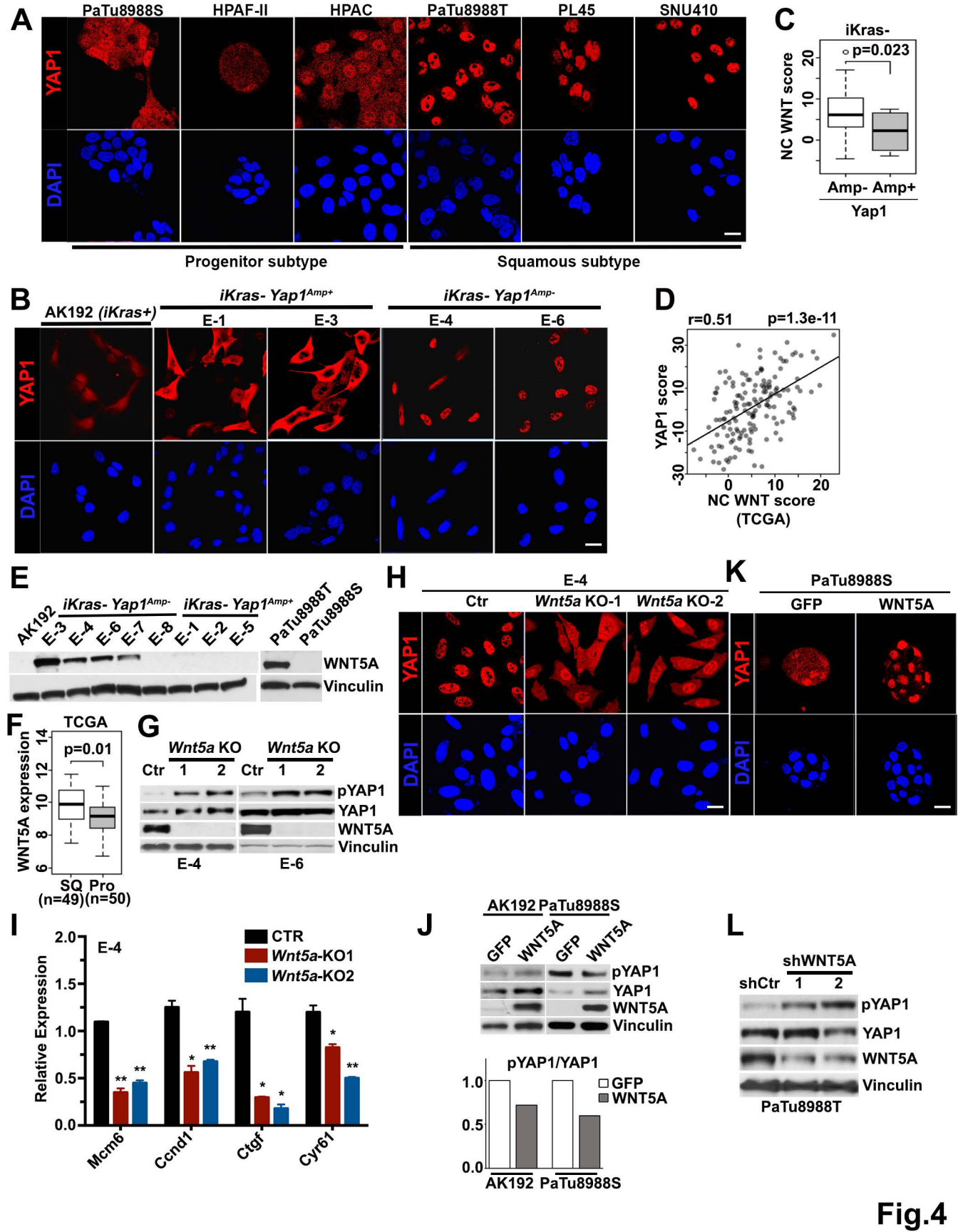
A
PaTu8988S
HPAF-II
HPAC
PaTu8988T
PL45
SNU410
YAP1
DAPI
Progenitor subtype
Squamous subtype
C
iKras-
p=0.023
NC WNT score
Amp- Amp+
Yap1
B
AK192 (iKras+)
iKras- Yap1Amp+
iKras- Yap1Amp-
E-1
E-3
E-4
E-6
D
r=0.51
p=1.3e-11
YAP1 score
NC WNT score
(TCGA)
E
AK192
iKras- Yap1Amp-
iKras- Yap1Amp+
PaTu8988T
PaTu8988S
E-3
E-4
E-6
E-7
E-8
E-1
E-2
E-5
WNT5A
Vinculin
F
TCGA
p=0.01
WNT5A expression
SQ Pro
(n=49)(n=50)
G
Wnt5a KO
Ctr
1
2
pYAP1
YAP1
WNT5A
Vinculin
E-4
E-6
H
E-4
Ctr
Wnt5a KO-1
Wnt5a KO-2
K
PaTu8988S
GFP
WNT5A
I
E-4
CTR
Wnt5a-KO1
Wnt5a-KO2
Relative Expression
Mcm6
Ccnd1
Ctgf
Cyr61
J
AK192 PaTu8988S
GFP
WNT5A
pYAP1
YAP1
WNT5A
Vinculin
pYAP1/YAP1
GFP
WNT5A
AK192 PaTu8988S
L
shWNT5A
shCtr
1
2
pYAP1
YAP1
WNT5A
Vinculin
PaTu8988T

Fig.4

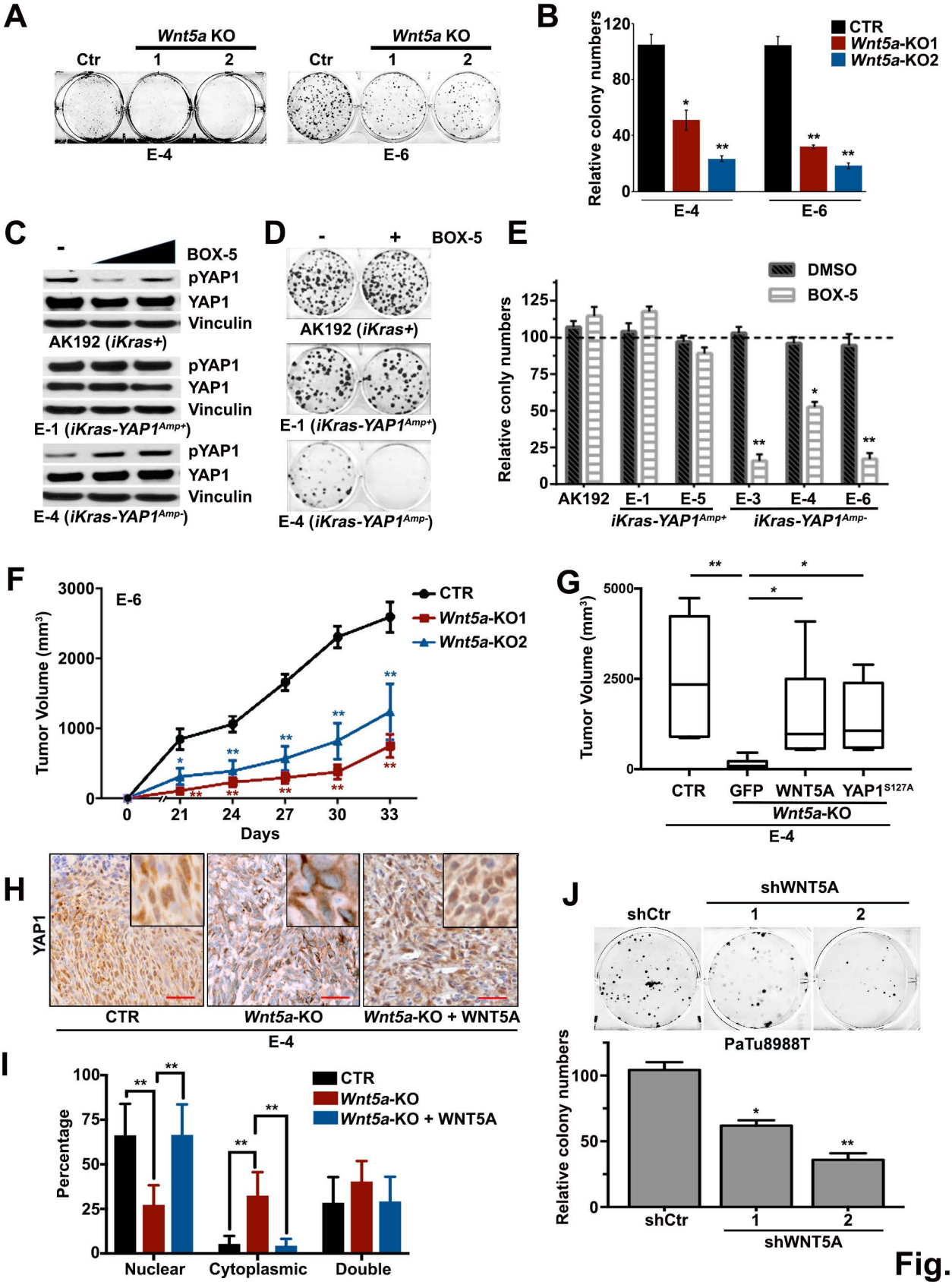
A
Wnt5a KO
Ctr
1
2
E-4
E-6
B
Relative colony numbers
CTR
Wnt5a-KO1
Wnt5a-KO2
C
BOX-5
pYAP1
YAP1
Vinculin
AK192 (iKras+)
E-1 (iKras-YAP1Amp+)
E-4 (iKras-YAP1Amp-)
D
BOX-5
E
Relative conly numbers
DMSO
BOX-5
AK192
E-1
E-5
E-3
E-4
E-6
iKras-YAP1Amp+
iKras-YAP1Amp-
F
E-6
Tumor Volume (mm3)
Days
CTR
Wnt5a-KO1
Wnt5a-KO2
G
Tumor Volume (mm3)
CTR
GFP
WNT5A
YAP1S127A
Wnt5a-KO
E-4
H
YAP1
CTR
Wnt5a-KO
Wnt5a-KO + WNT5A
E-4
I
Percentage
CTR
Wnt5a-KO
Wnt5a-KO + WNT5A
Nuclear
Cytoplasmic
Double
J
shCtr
shWNT5A
1
2
PaTu8988T
Relative colony numbers
shCtr
shWNT5A

Fig.5

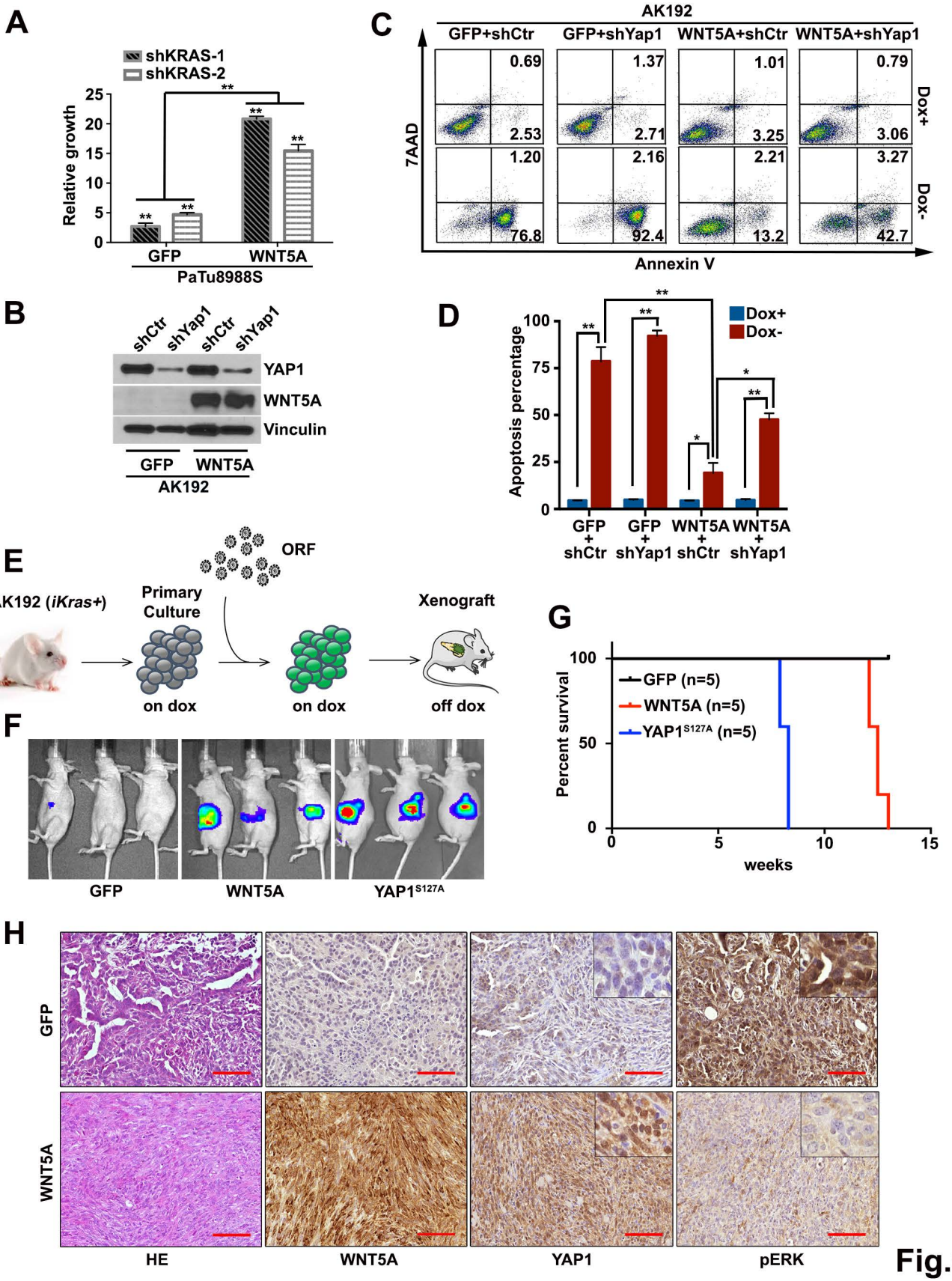
A
shKRAS-1
shKRAS-2
Relative growth
25
20
15
10
5
0
**
**
**
**
**
GFP
WNT5A
PaTu8988S
B
shCtr
shYap1
shCtr
shYap1
YAP1
WNT5A
Vinculin
GFP
WNT5A
AK192
C
AK192
GFP+shCtr
GFP+shYap1
WNT5A+shCtr
WNT5A+shYap1
0.69
1.37
1.01
0.79
2.53
2.71
3.25
3.06
1.20
2.16
2.21
3.27
76.8
92.4
13.2
42.7
Dox+
Dox-
7AAD
Annexin V
D
Dox+
Dox-
Apoptosis percentage
100
75
50
25
0
**
**
**
*
*
**
GFP + shCtr
GFP + shYap1
WNT5A + shCtr
WNT5A + shYap1
E
ORF
AK192 (iKras+)
Primary Culture
Xenograft
on dox
on dox
off dox
F
GFP
WNT5A
YAP1S127A
G
Percent survival
100
50
0
GFP (n=5)
WNT5A (n=5)
YAP1S127A (n=5)
0
5
10
15
weeks
H
GFP
WNT5A
HE
WNT5A
YAP1
pERK

Fig.6

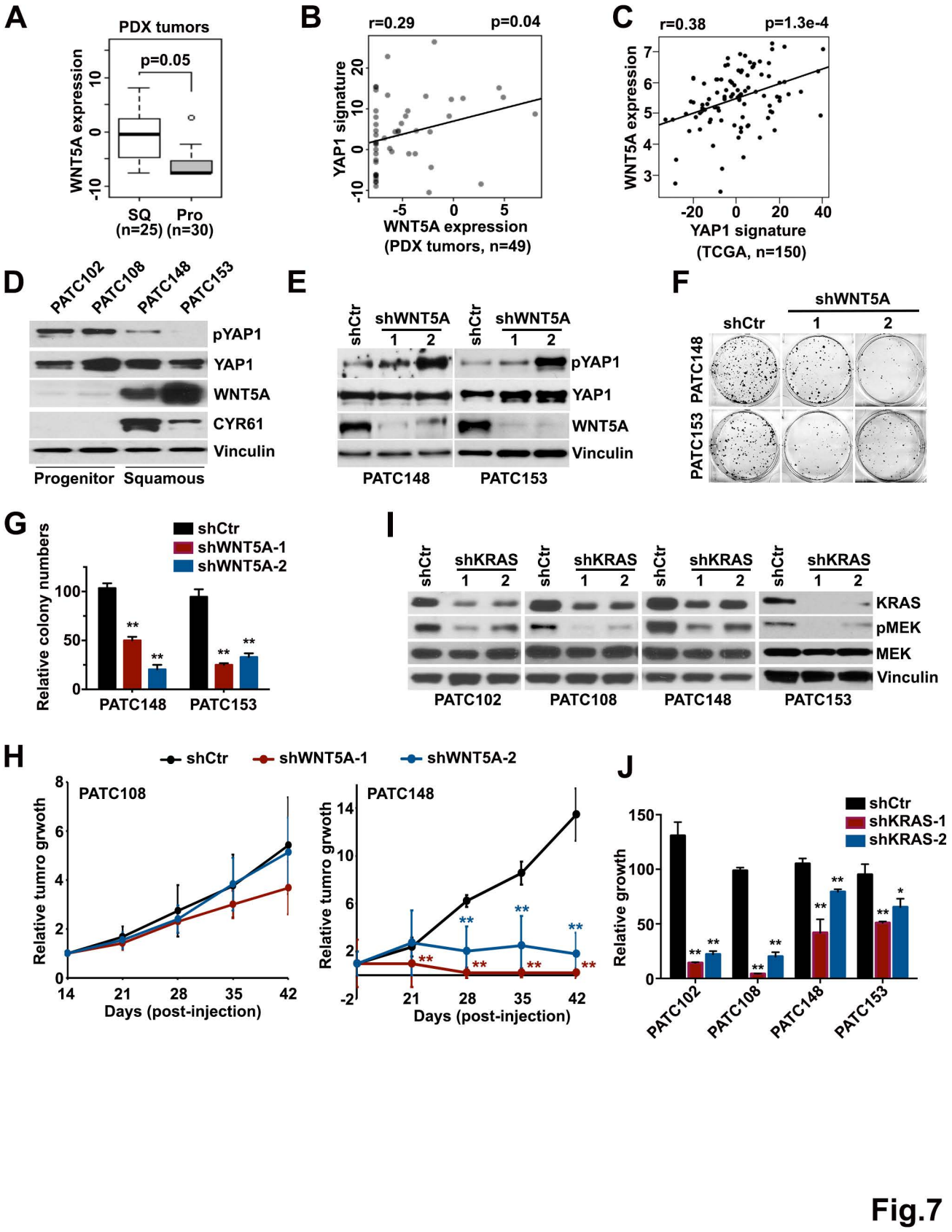
A
PDX tumors
p=0.05
WNT5A expression
SQ (n=25)
Pro (n=30)
B
r=0.29
p=0.04
YAP1 signature
WNT5A expression (PDX tumors, n=49)
C
r=0.38
p=1.3e-4
WNT5A expression
YAP1 signature (TCGA, n=150)
D
PATC102
PATC108
PATC148
PATC153
pYAP1
YAP1
WNT5A
CYR61
Vinculin
Progenitor
Squamous
E
shCtr
shWNT5A
1
2
pYAP1
YAP1
WNT5A
Vinculin
PATC148
PATC153
F
shCtr
shWNT5A
1
2
PATC148
PATC153
G
shCtr
shWNT5A-1
shWNT5A-2
Relative colony numbers
PATC148
PATC153
I
shCtr
shKRAS
1
2
KRAS
pMEK
MEK
Vinculin
PATC102
PATC108
PATC148
PATC153
H
shCtr
shWNT5A-1
shWNT5A-2
PATC108
PATC148
Relative tumro grwoth
Days (post-injection)
J
shCtr
shKRAS-1
shKRAS-2
Relative growth
PATC102
PATC108
PATC148
PATC153

Fig.7

Supplementary Materials and Method

Immunostaining and Western Blot Analysis

For immunofluorescence staining, mouse and human cells were fixed with 4% paraformaldehyde-PBS for 15 min. Following Triton-X100 permeabilization and blocking, cells were incubated with primary antibodies overnight at 4°C following with Alexa 594-conjugated secondary antibodies at 4°C for 1 hour (Thermo Fisher Scientific, 1:1000). Samples were mounted using VECTASHIELD Antifade Mounting Medium with DAPI (Vector Laboratories) and immunofluorescence was detected using Olympus confocal microscopy. For western blot analysis, cells were lysed on ice using RIPA buffer supplemented with protease and phosphatase inhibitors (Sigma).

Primary Antibodies for Immunostaining and Western Blot Analysis: Yap (#14074, Cell Signaling), pYAP (#4911, Cell Signaling), Lats1 (#3477, Cell Signaling), pLats1(#8654, Cell Signaling), Mst1 (#3682, Cell Signaling), Mst2 (#3952,Cell Signaling), p-MST1/2 (#3681, Cell Signaling), Merlin(#12888, Cell Signaling), Phospho-Merlin (#13281,Cell Signaling), Wnt5a (#2530, Cell Signaling), Ki-67 (VP-K451, Vector Laboratories), Cyr61 (sc-13100, Santa Cruz Biotechnology), CTGF (sc-14939, Santa Cruz Biotechnology), AXL (8661, Cell Signaling), pErk (4376, Cell Signaling), pMEK (4376, Cell Signaling), Ck-19 (16858-1-AP, Proteintech), Actin (A2228, Sigma Aldrich), Vinculin (V4139, Sigma Aldrich), Kras (sc-30, Santa Cruz Biotechnology).

Ectopic expression of YAP1 and WNT5A in mouse and human cells

To generate $YAP1^{S127A}$-expressing stable Pa04C cells, Pa04C cells were transfected with a linearized pcDNA3.1 plasmid with or without YAP1 cDNA containing S127A substitution. Two days post-transfection using Lipofectamine1000, cultures were selected in G418 (Sigma) and single clones were picked and expanded for further analysis. Overexpression of YAPS127A or WNT5A in human or mouse cells other than Pa04C were acheieved with lentivral infection.

Briefly, lentivirus infection was performed by transfecting 293T cells with either GFP control, $YAP1^{S127A}$, or WNT5A cloned in pHAGE lentivirus vector {EF1α promoter-GW-IRES-eGFP (GW: Gateway modified)}. The virus was concentrated using ultracentrifuge and added to target cells in a 6-well plate containing 10ug/ml of polybrene (Millipore). 48 hours after infection GFP positive cells were selected by flow sorting.

Lentivirus Mediated shRNA Knockdown

The clone IDs for shRNA are as follows: sh_mouse Yap1-1 (TRCN0000238436), sh mouse Yap1-2 (TRCN0000095864), sh_huYap1-1 (TRCN0000107265), sh_huYap1-2 (TRCN0000107266), sh_huWnt5a-1 (TRCN0000062717), sh_huWnt5a-2 (TRCN0000288987), sh_hu Kras-1 (TRCN0000033260), sh_hu Kras-2 (TRCN0000033262).

Crispr-Cas9 Mediated Gene Knockout

Sequences for *Wnt5a* sgRNA are as follows:

sgRNA-1 F: CTTGAGAAAGTCCTGCCAGT; R: ACTGGCAGGACTTTCTCAAG.

sgRNA-2 F: GAAACTCTGCCACTTGTATC; R: GATACAAGTGGCAGAGTTTC.

sgRNA-3 F: TATACTTCTGACATCTGAAC; R: GTTCAGATGTCAGAAGTATA.

sgRNA-4 F: ACAGCCTCTCTGCAGCCAAC, R: GTTGGCTGCAGAGAGGCTGT.

Sequences for *Yap1* sgRNA are as follows:

sgRNA-1 F: ACCAGGTCGTGCACGTCCGC; R: GCGGACGTGCACGACCTGGT.

sgRNA-2 F: CCCCGCGGACGTGCACGACC; R: GGTCGTGCACGTCCGCGGGG.

Xenograft Studies

For orthotopic xenografts, 5×10^5 cells were injected pancreatically into NCr nude mice (Taconic) and tumor growth was monitored with bioluminescent imaging as described[1]. For Sub-Q xenografts, 1×10^6 cells (mouse tumor cells) or 3×10^6 cells (human PDAC or PDX cells) were

injected subcutaneously into the lower flank of NCr nude mice. Tumor volumes were measured every 7 days starting from Day 7 post injection and calculated using the formula, volume = length × width^2/2.

Immunoprecipitation Assay

Immunoprecipitation of YAP1 complexes was performed by lysing cells with 1% NP40 lysis buffer containing phosphatase and protease inhibitor cocktails on ice for 45 minutes. 1 mg of lysate was incubated overnight at 4ºC with primary antibodies followed with protein A/G Plus-agarose (sc-2003, Santa Cruz) for 3 hours at 4ºC. Immunoprecipitates were washed three times with lysis buffer, then re-suspended with 2X sample buffer boiled for 5 min and detected by western blot analyses.

Quantitative Real-time Polymerase Chain Reaction Analysis

RNA from cell lines and pancreas tissues was isolated using RNeasy Mini Kit (Qiagen) and first-strand cDNA was synthesized from 2 µg total RNA using random primers and Omniscript® Reverse Transkriptase Kit (Qiagen). Actin was used as housekeeping gene. Real-time polymerase chain reaction experiments were performed in triplicates and are displayed ± SD.

Clonogenic assay

500-2000 cells were seeded into each well of 6-well plate in triplicates and incubated to allow colony formation for 10-20 days. The colonies were stained with 0.2% crystal violet in 80% methanol for 30 minutes at room temperature and de-stained upon which they were scanned and colonies counted using Image J (http://rsb.info.nih.gov/ij/).

Gene Expression and PDAC-Subtype Analysis

mRNA expression profiling on Illumina microarrays were performed according to the manufacture's protocol. Raw data was processed using Genome Studio (GSGX Version 1.6.0) and

analysis was done using group quantile normalization with background subtraction. The software package LIMMA (Linear Models for Microarray Data) was applied to detect significantly differentially expressed probes using Benjamini-Hochberg adjusted p-values. For GSEA analysis, gene sets collection from MSigDB 3.0 and Kyoto Encyclopedia of Genes and Genomes (KEGG) were included in the analysis.

For molecular subtype analysis, we combined subtype specific genes from Collisson et al and Bailey et al studies to construct a "NanoString signature" comprised of 32, 23, and 17 subtype specific genes for squamous, progenitor, and ADEX subtypes, respectively (see supplementary table 7). To call PDAC subtypes in human PDAC cell lines or PDXs, we used the following algorithm. First, subtype signature scores were calculated by summing up Z scores from subtype specific genes which were ceiled at 2.5 and bottomed at -0.5. Kmeans two separation were then done to call high and low groups within each subtype. SQ/Pro subtypes are then called as squamous gene high/progenitor gene low and vice versa. ADEX subtype is called as ADEX gene high and SQ/Pro gene low. The remaining tumors are undefined. The nanoString call results are further confirmed by heatmap visualiation using Collission genes (data not shown)[2]. The clusters were viewed using Java TreeView (version 1.1.6r4) [3].

Supplementary Reference

1. Kapoor A, Yao W, Ying H, et al. Yap1 activation enables bypass of oncogenic Kras addiction in pancreatic cancer. *Cell* 2014;158(1):185-97. doi: 10.1016/j.cell.2014.06.003 [published Online First: 2014/06/24]

2. Collisson EA, Sadanandam A, Olson P, et al. Subtypes of pancreatic ductal adenocarcinoma and their differing responses to therapy. *Nat Med* 2011;17(4):500-3. doi: 10.1038/nm.2344 [published Online First: 2011/04/05]

3. Saldanha AJ. Java Treeview--extensible visualization of microarray data. *Bioinformatics* 2004;20(17):3246-8. doi: 10.1093/bioinformatics/bth349

Supplementary Figure Legends

Figure S1. YAP1 is essential for PDAC development.

(A) *Yap1* wild-type (YAP-WT) or knockout (YAP-KO) $Kras^{G12D}$;$Trp53^{R172H}$ mice driven by *Mist1-Cre*^{ERT2} upon tamoxifen injection. Pacreata were collected at indicated time points and stained for Ki-67 to assess cell proliferation. Scale bar: 100μm. (B) *Yap1* wild-type (YAP-WT) or knockout (YAP-KO) $Kras^{G12D}$;$Trp53^{R172H}$ mice driven by *Elastase-Cre*^{ERT2} upon tamoxifen injection. Pacreata collected at 4 months post-injection and stained for H&E (Top) shows complete block of tumor development and relative normal pancreatic architecture in YAP-KO mice in contrast with ductal adenocarcinoma in YAP-WT mice. (Bottom) Immunostaining for YAP shows strong nuclear staining in tumor epithelia of YAP-WT pancreata while showing complete lack of expression in YAP-KO mice. Scale bar: 100μm.

Figure S2. YAP1 enhances the malignant phenotypes of PDAC and is activated in squamous subtype.

(A) In vitro wound healing assay for Pa04C cells expressing YAP1^{S127A} or control vector (Vec) showing more aggressive migration of Pa04C-YAP1^{S127A} cells. (B) Representative gross images of orthotopic tumors from Pa04C-Vector (Vec) or Pa04C-YAP^{S127A} cells. Top: uncut tumors; Bottom: tumors were cut in half to reveal necrotic area. (C) Quantification of necrotic area. **: $p<0.01$. (D) Orthotopic xenograft tumors from Pa04C cells expressing vector (Vec) or YAP1^{S127A} were stained for known YAP1-target genes CYR61, CTGF and AXL. Scale bar: 100μm. (E) Relative mRNA levels of *YAP1*, indicated YAP1-target genes and genes related with EMT in Pa04C cells expressing vector (Vec) or YAP1^{S127A}. Error bars indicate ±SD of triplicates. **: $p<0.01$. (F) GSEA plot of YAP1 activation signature based on the gene expression profiles of vector- vs YAP1^{S127A}-expressing Pa04C cells. NES denotes normalized enrichment score. (G-H)

Clustering of human PDAC cell lines (G) and human PDXs (H) based on subtype-specific gene signatures. Heatmap of squamous (SQ), progenitor (PRO) subtype, YAP1 activation signature and WNT5A gene expression is shown. Asterisk: cell lines used in this study. (I) Heatmap shows the expression level of squamous (SQ) and progenitor (Pro) subtype signature genes measured with NanoString in PaTu8988S cells expressing GFP or $YAP1^{S127A}$ and PaTu8988T cells. (J) Expression changes of squamous (SQ) or progenitor (Pro) subtype genes in Pa04C-Vector or Pa04C-YAPS127A tumors. Results were presented as log2 ratio between $YAP1^{S127A}$ and Vector groups.

Figure S3. YAP1 is required for squamous subtype PDACs.

(A) Western blot analysis for YAP1 in PaTu8988S and PaTu8988T cells engineered with inducible shRNA targeting YAP1 in the presence or absence of doxycycline for 72 hours. Inducible non-targeting shRNA (ishCtr) was used as control. (B) PaTu8988S and PaTu8988T cells engineered with inducible shRNA targeting YAP1 were subcutaneously injected into nude mice. Inducible non-targeting shRNA (ishCtr) was used as control. Animals were treated with doxycycline once tumor size reached 20-50 mm^3. Tumor volumes were measured on the indicated dates post-injection. Results are presented as the means±SEM. (n=5). (C) Western blot analysis for KRAS, phosphor-MEK1/2 and MEK1/2 in PaTu8988S cells expressing GFP or $YAP1^{S127A}$ and PaTu8988T cells upon knockdown of KRAS with two independent shRNAs. Non-targeting shRNA (shCtr) was used as control. (D) GSEA plots show genes induced upon KRAS knockdown or suppressed upon KRAS expression are enriched in squamous subtype human PDAC. (E) Heatmap shows the expression of KRAS-independence gene signature among human PDAC subtypes in ICGC dataset. S: squamous subtype; A: ADEX subtype; P: progenitor subtype; I: immunogenic subtype. (F) Cellular proliferation of mouse PDAC cells infected with two

independent shRNAs targeting Yap1 or non-targeting shRNA (shCtr). Quantification from triplicates is shown. **: p<0.01. (G) Two independent *iKras- Yap1*$^{Amp-}$ cell lines were infected with two independent shRNAs targeting Yap1 or non-targeting shRNA (shCtr). Cells were cultured in the presence or absence of doxycycline for 48 hours and cell lysates were subjected to western blot analysis for YAP1, phosphor-ERK and ERK. (H) Representative images of the colony formation assay upon Yap1 knockdown in *iKras- Yap1*$^{Amp-}$ cell lines grown in the presence or absence of doxycycline. Non-targeting shRNA (shCtr) was used as control. Quantification of colony formation is shown in (I) and is presented as relative colony numbers upon normalization to shCtr group. Error bars represent ±SD of triplicate wells, **: p<0.01.

Figure S4. YAP1 is activated in squamous subtype PDAC

(A) Mutation and copy number alteration (CAN) requency of *YAP1* in human PDAC from ICGC and TCGA datasets. (B) *Yap1* gene amplification status in *iKras*- tumors. (C) mRNA expression level of YAP1 in human PDAC cell lines. (D) *iKras*+, *iKras- Yap1*$^{Amp-}$ and *iKras- Yap1*$^{Amp+}$ tumors were stained for YAP1. (E) Equal amount of YAP1 protein was immunoprecipitated from human PDAC cell lines of indicated subtypes and subjected to western blot analysis for phosphor-YAP1 (S127) and YAP1 (top). Input shows the western blot analysis for YAP1, phosphor-LATS1/2, LATS1/2, phosphor-MST1/2, MST1/2 and WNT5A in whole cell lysates (bottom). Quantification of phosphor-LAST1/2 to total LATS1/2 ratio or phosphor-MST1/2 to total MST1/2 ratio was shown in (F) and (G) respectively. (H) Equal amount of YAP1 or LATS1/2 protein was immunoprecipitated from mouse *iKras*- PDAC cells and subjected to western blot analysis for phosphor-YAP1 (S127) and YAP1, or phosphor-LATS1/2 and LATS1/2 (top). Input shows the western blot analysis for phosphor-MST1/2, MST1, MST2, LATS1/2 and YAP1 in whole cell lysates (bottom).

Figure S5. WNT5A overexpression contributes to YAP1 activation

(A) Correlation between non-canonical WNT signature and YAP1 signature in PDAC ICGC dataset. (B) Relative mRNA levels of indicated WNT ligands in mouse *iKras*- PDAC cells. Error bars indicate ±SD of triplicates. (C) *WNT5A* expression in squamous (SQ) or progenitor (Pro) subtype human PDACs in ICGC dataset. (D-E) Expression of *Yap1* (D) or subtype-specific genes (E) in subcutaneous xenograft tumors generated with E-4 (*iKras*- *Yap1*$^{Amp-}$) and E4-*Wnt5a* KO cells infected with GFP or WNT5A.

Figure S6. WNT5A overexpression leads to the bypass of KRAS-dependency

(A) Representative images of the colony formation assay in mouse AK192 (*iKras*+) cells infected with GFP or WNT5A grown in the presence (Dox+) or absence (Dox-) of doxycycline. Quantification of colony formation from triplicates is shown in (B). Error bars from all panels indicate ±SD. *: $p<0.05$. (C) Western blot analysis for YAP1 and WNT5A in AK192 or AK192-*Yap1* KO cells infected with GFP or WNT5A. (D) AK192 or AK192-*Yap1* KO cells expressing luciferase were infected with lentivirus expressing GFP or WNT5A and orthotopically injected into nude mice pancreas in the presence of doxycycline. Animals were withdrawn from doxycycline four days later and tumor growth was visualized by bioluminescent imaging at 6 weeks.

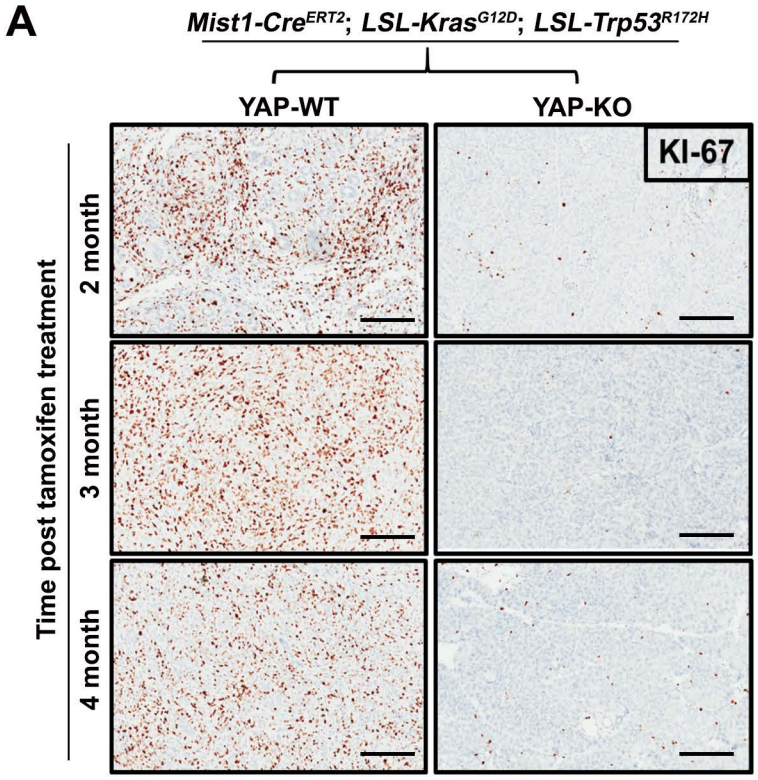
A
Mist1-Cre^ERT2; LSL-Kras^G12D; LSL-Trp53^R172H
YAP-WT
YAP-KO
KI-67
Time post tamoxifen treatment
2 month
3 month
4 month

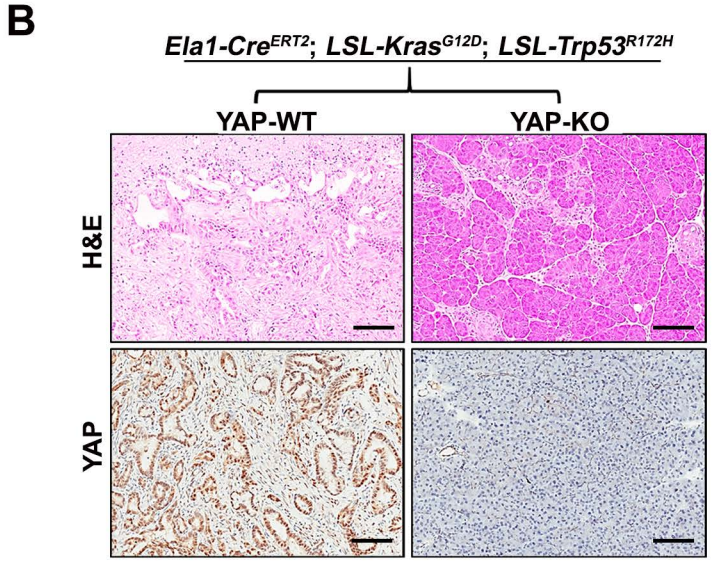
B
Ela1-Cre^ERT2; LSL-Kras^G12D; LSL-Trp53^R172H
YAP-WT
YAP-KO
H&E
YAP

Fig. S1

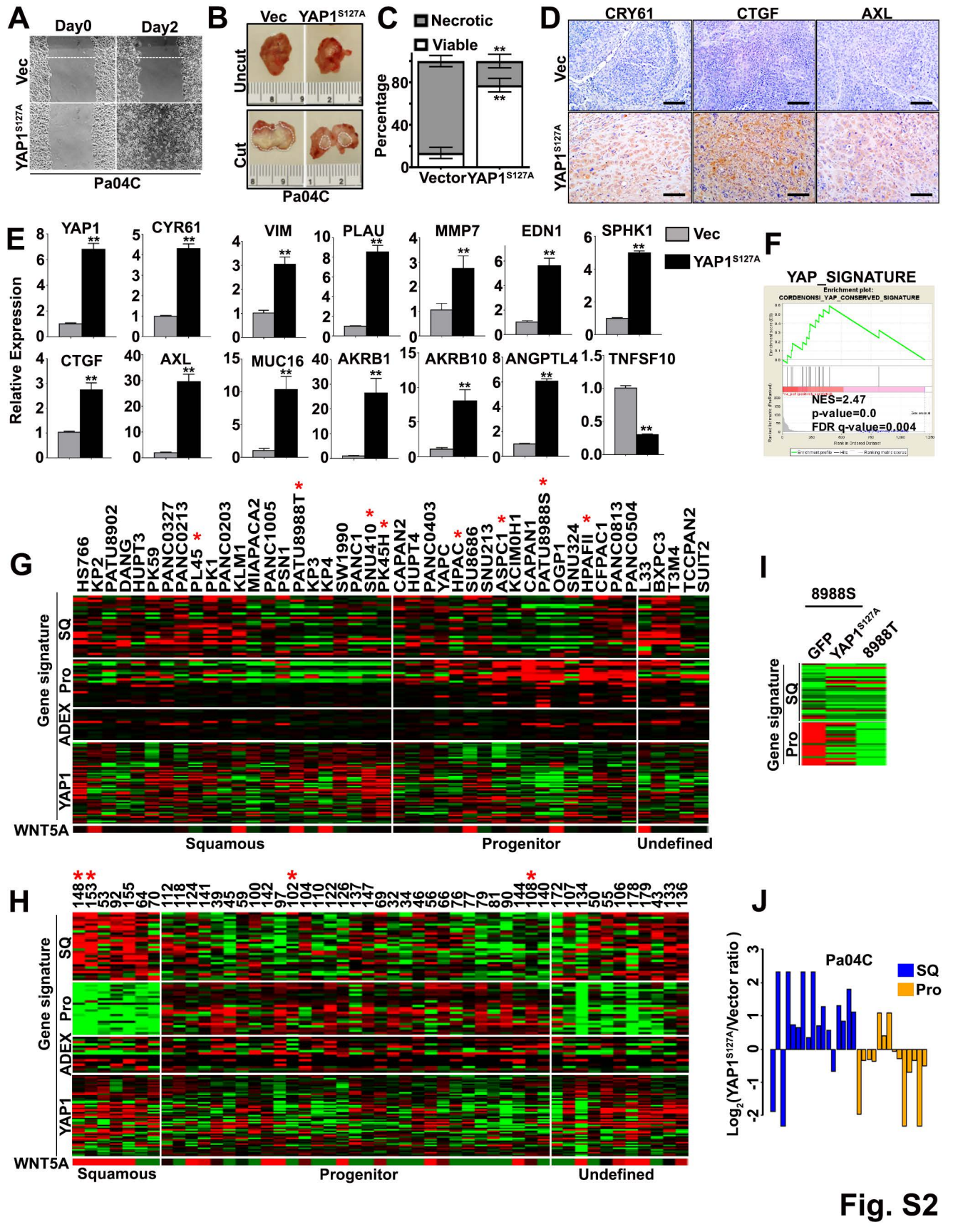
A
Day0
Day2
Vec
YAP1S127A
Pa04C
B
Vec
YAP1S127A
Uncut
Cut
Pa04C
C
Necrotic
Viable
Percentage
Vector
YAP1S127A
D
CRY61
CTGF
AXL
Vec
YAP1S127A
E
Relative Expression
YAP1
CYR61
VIM
PLAU
MMP7
EDN1
SPHK1
CTGF
AXL
MUC16
AKRB1
AKRB10
ANGPTL4
TNFSF10
Vec
YAP1S127A
F
YAP_SIGNATURE
Enrichment plot:
CORDENONSI_YAP_CONSERVED_SIGNATURE
NES=2.47
p-value=0.0
FDR q-value=0.004
G
HS766
KP2
PATU8902
DANG
HUPT3
PK59
PANC0327
PANC0213
PL45
PK1
PANC0203
KLM1
MIAPACA2
PANC1005
PSN1
PATU8988T
KP3
KP4
SW1990
PANC1
SNU410
PK45H
CAPAN2
HUPT4
PANC0403
YAPC
HPAC
SU8686
SNU213
ASPC1
KCIM0H1
CAPAN1
PATU8988S
OGP1
SNU324
HPAFII
CFPAC1
PANC0813
PANC0504
L33
BXPC3
T3M4
TCCPAN2
SUIT2
Gene signature
SQ
Pro
ADEX
YAP1
WNT5A
Squamous
Progenitor
Undefined
I
8988S
GFP
YAP1S127A
8988T
Gene signature
SQ
Pro
H
Gene signature
SQ
Pro
ADEX
YAP1
WNT5A
Squamous
Progenitor
Undefined
J
Pa04C
SQ
Pro
Log2(YAP1S127A/Vector ratio)

Fig. S2

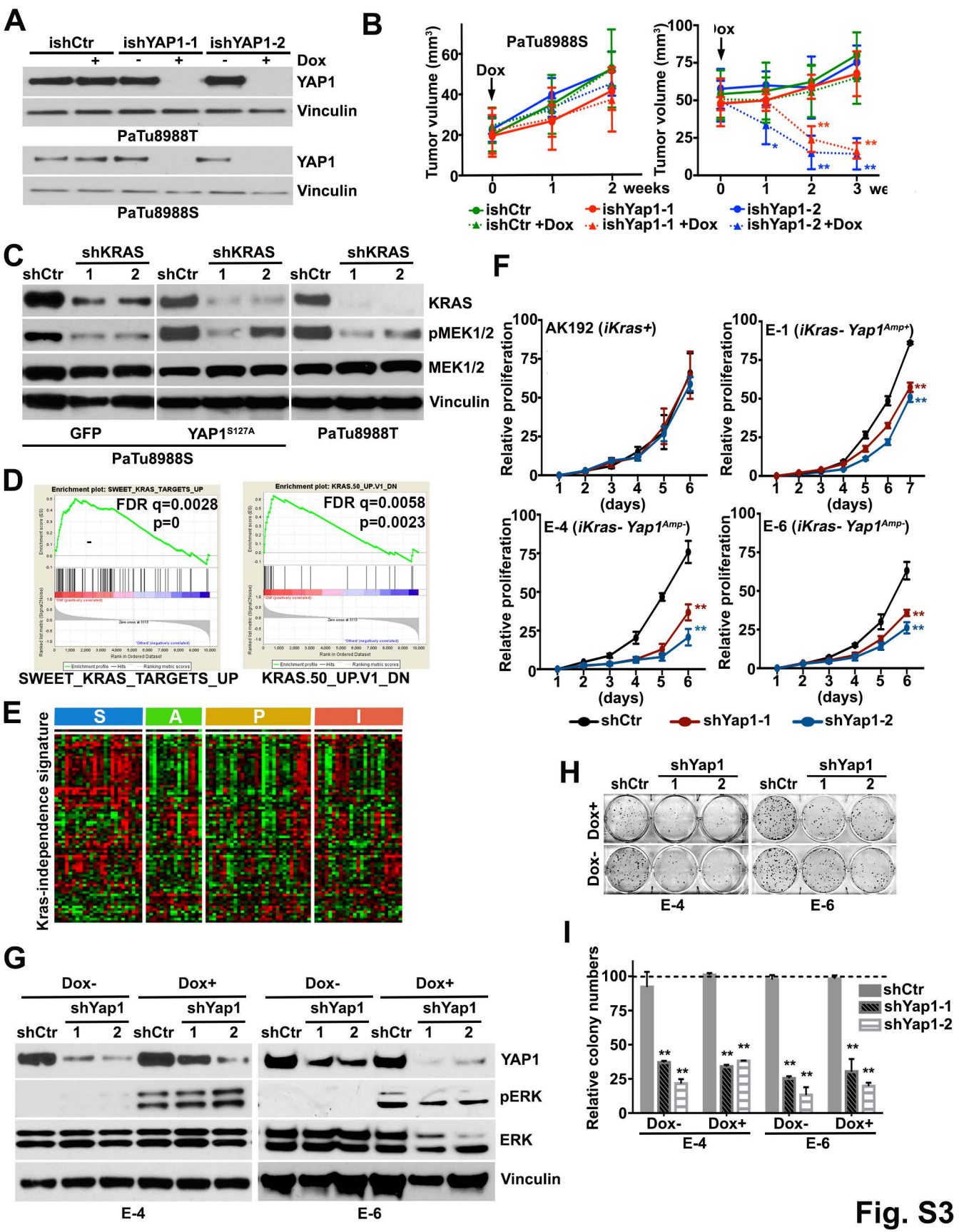
A
ishCtr
ishYAP1-1
ishYAP1-2
Dox
YAP1
Vinculin
PaTu8988T
PaTu8988S
B
PaTu8988S
Dox
Tumor vulume (mm3)
weeks
ishCtr
ishCtr +Dox
ishYap1-1
ishYap1-1 +Dox
ishYap1-2
ishYap1-2 +Dox
C
shKRAS
shCtr
KRAS
pMEK1/2
MEK1/2
Vinculin
GFP
YAP1S127A
PaTu8988T
PaTu8988S
D
Enrichment plot: SWEET_KRAS_TARGETS_UP
FDR q=0.0028
p=0
SWEET_KRAS_TARGETS_UP
Enrichment plot: KRAS.50_UP.V1_DN
FDR q=0.0058
p=0.0023
KRAS.50_UP.V1_DN
E
S
A
P
I
Kras-independence signature
F
AK192 (iKras+)
E-1 (iKras- Yap1Amp+)
E-4 (iKras- Yap1Amp-)
E-6 (iKras- Yap1Amp-)
Relative proliferation
(days)
shCtr
shYap1-1
shYap1-2
G
Dox-
Dox+
shYap1
shCtr
YAP1
pERK
ERK
Vinculin
E-4
E-6
H
shYap1
shCtr
Dox+
Dox-
E-4
E-6
I
Relative colony numbers
shCtr
shYap1-1
shYap1-2
Dox-
Dox+
E-4
E-6

Fig. S3

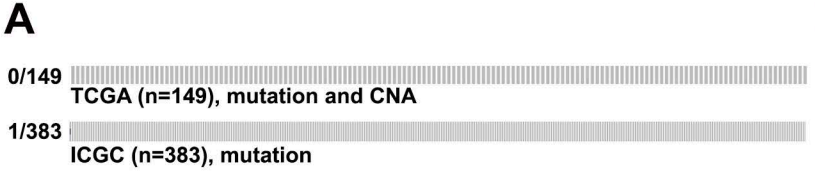

B

iKras- escapers	*Yap1* Amplification
E-1	+
E-2	+
E-3	-
E-4	-
E-5	+
E-6	-
E-7	-
E-8	-

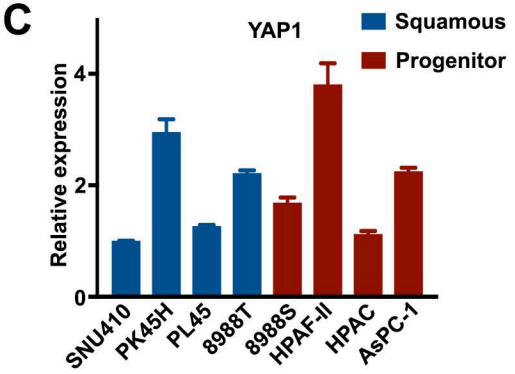

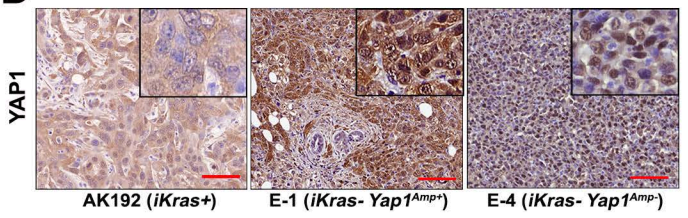

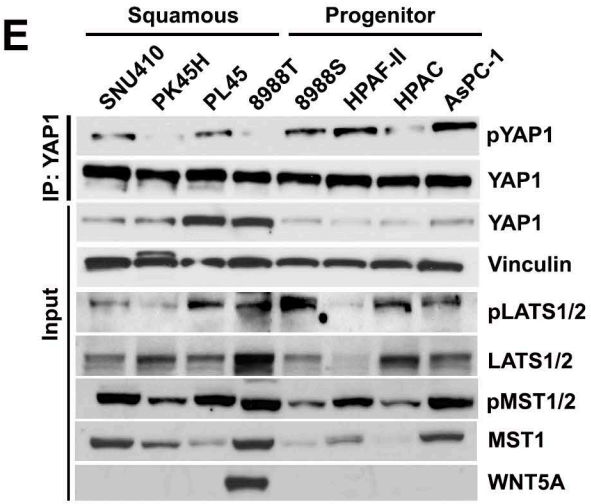

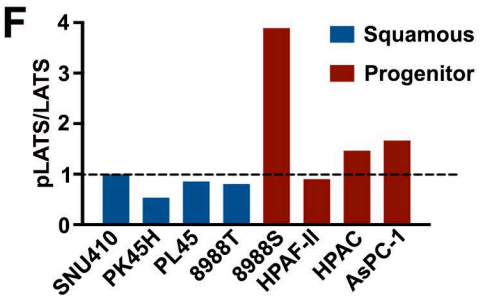

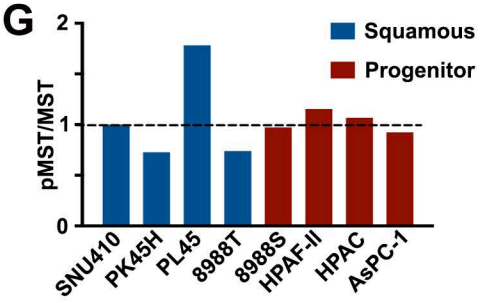

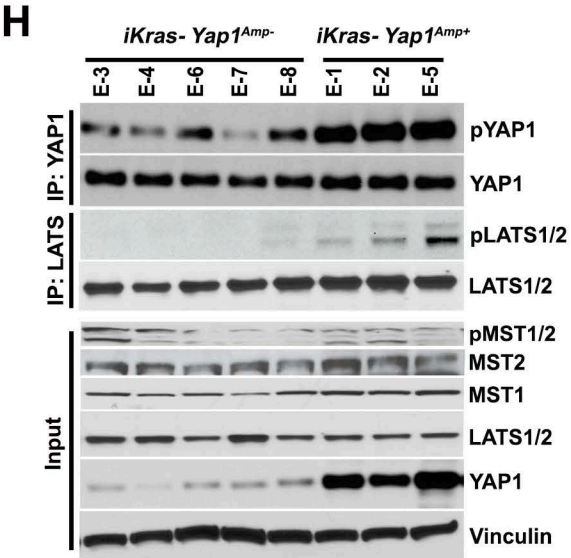

Fig.S4

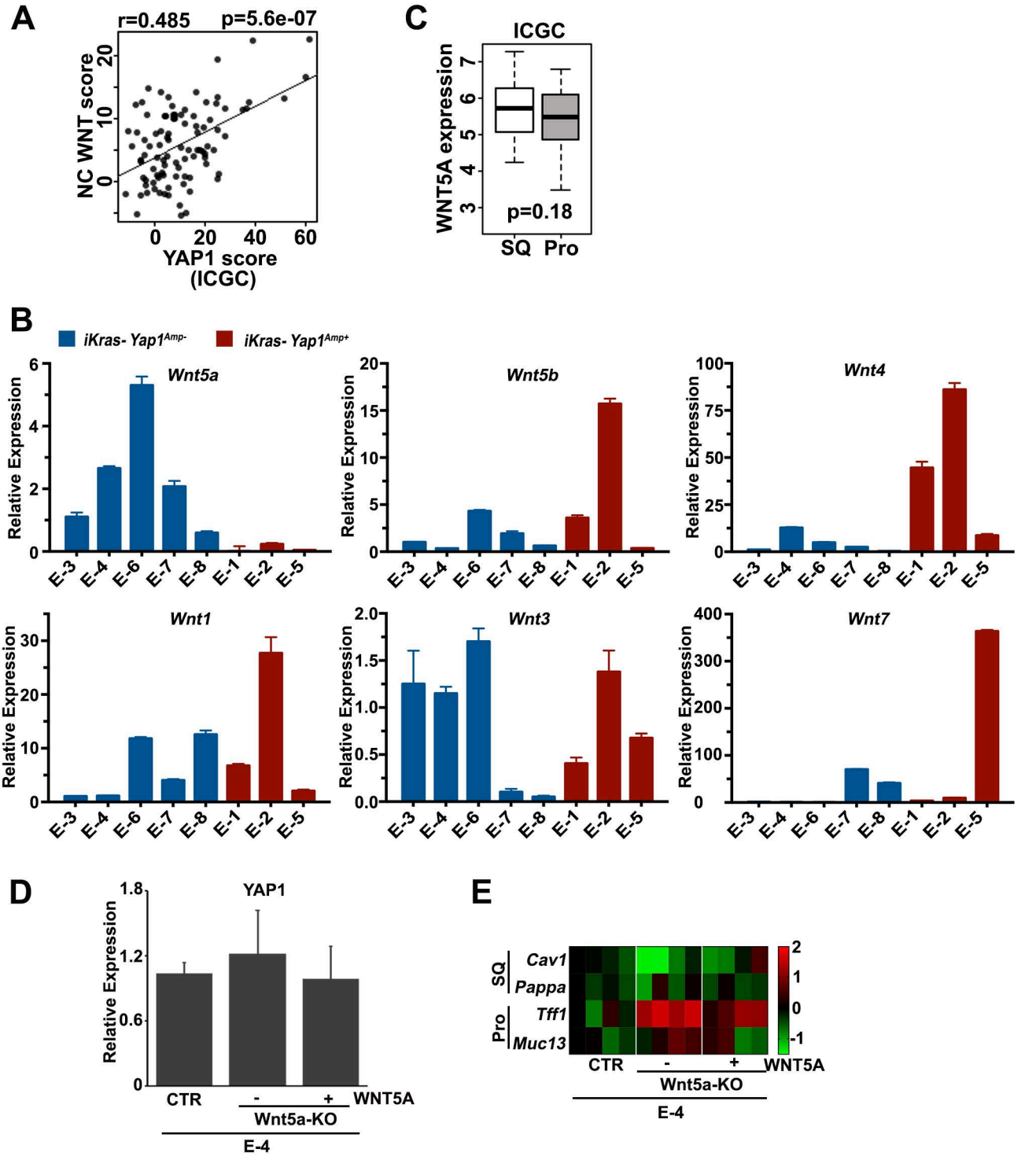
A
r=0.485
p=5.6e-07
NC WNT score
YAP1 score
(ICGC)
C
ICGC
WNT5A expression
p=0.18
SQ
Pro
B
iKras- Yap1Amp-
iKras- Yap1Amp+
Wnt5a
Wnt5b
Wnt4
Wnt1
Wnt3
Wnt7
Relative Expression
E-3
E-4
E-6
E-7
E-8
E-1
E-2
E-5
D
YAP1
Relative Expression
CTR
-
+
WNT5A
Wnt5a-KO
E-4
E
SQ
Pro
Cav1
Pappa
Tff1
Muc13
CTR
-
+
WNT5A
Wnt5a-KO
E-4

Fig. S5

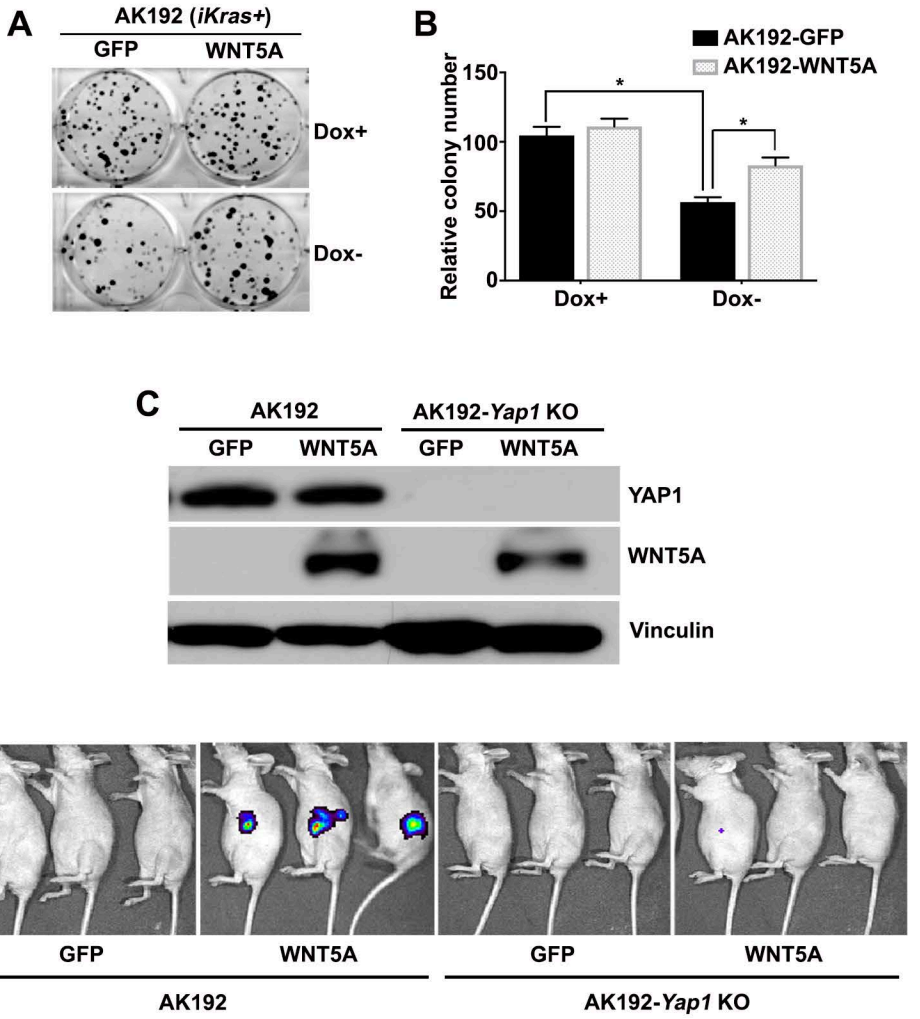
A
AK192 (iKras+)
GFP
WNT5A
Dox+
Dox-
B
AK192-GFP
AK192-WNT5A
Relative colony number
150
100
50
0
*
*
Dox+
Dox-
C
AK192
AK192-Yap1 KO
GFP
WNT5A
GFP
WNT5A
YAP1
WNT5A
Vinculin
D
GFP
WNT5A
GFP
WNT5A
AK192
AK192-Yap1 KO

Fig. S6

Supplementary Table 1. Sample information for human PDAC cell lines and PDX lines

Name	KRAS mutations status	Molecular Subtype	Tumor Site	AJCC Stage	Differentiation
SNU-410	KRAS_G12D	Squamous			
PK45H	KRAS_G12D	Squamous			
PL45	KRAS_G12D	Squamous			
PaTu 8988T	KRAS_G12V	Squamous			
PaTu 8988S	KRAS_G12V	Progenitor			
HPAC	KRAS_G12D	Progenitor			
HPAFII	KRAS_G12D	Progenitor			
ASPC-1	KRAS_G12D	Progenitor			
MDA-PATC102	HRAS_G12D	Progenitor	Pancreatic body	IV	Poor
MDA-PATC108	KRAS_G12D	Progenitor	Pancreatic head	IIA	Poor
MDA-PATC148	KRAS_G12D	Squamous	Liver	IV	n/a
MDA-PATC153	WT	Squamous	Pancreatic body	IIB	Poor

Supplementary Table 2. YAP1-regulated genes are enirched in signatures for tumor development and metastasis.

NAME	SIZE	ES	NES	NOM p-val	FDR q-val
SHEDDEN_LUNG_CANCER_POOR_SURVIVAL_A6	60	0.50	4.45	0.00000	0.00000
VECCHI_GASTRIC_CANCER_EARLY_UP	61	0.46	4.24	0.00000	0.00000
ROSTY_CERVICAL_CANCER_PROLIFERATION_CLUSTER	41	0.53	4.09	0.00000	0.00000
SARRIO_EPITHELIAL_MESENCHYMAL_TRANSITION_UP	40	0.52	3.94	0.00000	0.00000
RODRIGUES_THYROID_CARCINOMA_POORLY_DIFFERENTIATED_UP	59	0.44	3.92	0.00000	0.00000
WHITEFORD_PEDIATRIC_CANCER_MARKERS	24	0.54	3.18	0.00000	0.00000
ZHANG_BREAST_CANCER_PROGENITORS_UP	31	0.48	3.12	0.00000	0.00000
SENGUPTA_NASOPHARYNGEAL_CARCINOMA_UP	33	0.44	2.98	0.00000	0.00002
WINNEPENNINCKX_MELANOMA_METASTASIS_UP	21	0.53	2.93	0.00000	0.00000
GRADE_COLON_CANCER_UP	60	0.32	2.84	0.00000	0.00002
BIDUS_METASTASIS_UP	20	0.51	2.79	0.00000	0.00006
TURASHVILI_BREAST_DUCTAL_CARCINOMA_VS_LOBULAR_NORMAL_DN	10	0.71	2.77	0.00000	0.00006
WU_CELL_MIGRATION	36	0.39	2.77	0.00000	0.00006
RHODES_UNDIFFERENTIATED_CANCER	12	0.65	2.72	0.00000	0.00008
ZHENG_GLIOBLASTOMA_PLASTICITY_UP	42	0.35	2.71	0.00000	0.00008
GRADE_COLON_AND_RECTAL_CANCER_UP	27	0.44	2.68	0.00000	0.00017
CHIANG_LIVER_CANCER_SUBCLASS_PROLIFERATION_UP	28	0.42	2.63	0.00000	0.00029
SCHUETZ_BREAST_CANCER_DUCTAL_INVASIVE_UP	44	0.34	2.62	0.00000	0.00036
PATIL_LIVER_CANCER	77	0.25	2.45	0.00000	0.00127
HALLMARK_EPITHELIAL_MESENCHYMAL_TRANSITION	36	0.347	2.44	0.00000	0.00109
ACEVEDO_LIVER_TUMOR_VS_NORMAL_ADJACENT_TISSUE_UP	59	0.26	2.33	0.00000	0.00274
LIEN_BREAST_CARCINOMA_METAPLASTIC_VS_DUCTAL_UP	12	0.55	2.33	0.00000	0.00279
PROVENZANI_METASTASIS_UP	17	0.46	2.28	0.00213	0.00375
WOO_LIVER_CANCER_RECURRENCE_UP	16	0.45	2.16	0.00000	0.00695
WANG_ESOPHAGUS_CANCER_VS_NORMAL_UP	17	0.44	2.22	0.00000	0.00485
HUMMERICH_SKIN_CANCER_PROGRESSION_UP	14	0.49	2.21	0.00000	0.00523
RAMALHO_STEMNESS_UP	12	0.50	2.12	0.00000	0.00843
RICKMAN_TUMOR_DIFFERENTIATED_WELL_VS_MODERATELY_DN	10	0.54	2.03	0.00195	0.01402
BORCZUK_MALIGNANT_MESOTHELIOMA_UP	22	0.36	2.01	0.00593	0.01498
OSMAN_BLADDER_CANCER_UP	21	0.35	1.97	0.00380	0.01835
PECE_MAMMARY_STEM_CELL_UP	12	0.47	1.94	0.00777	0.02192
JAEGER_METASTASIS_UP	13	0.45	1.93	0.00195	0.02232
DELYS_THYROID_CANCER_UP	51	0.23	1.89	0.00616	0.02703
ALONSO_METASTASIS_UP	12	0.40	1.69	0.03143	0.06335
VECCHI_GASTRIC_CANCER_ADVANCED_VS_EARLY_UP	20	0.30	1.60	0.04952	0.09008
LIAO_METASTASIS	48	0.19	1.59	0.03106	0.09390

Supplementary Table 3. YAP1-regulated genes are enriched in signatures related to cell proliferation and cell cycle progression, part of GP2 and GP4 gene programs associated with squamous subtype of PDAC* (Bailey et al).

NAME	SIZE	ES	NES	NOM p-val	FDR q-val
CHANG_CYCLING_GENES	39.00	0.54	4.03	0.00000	0.00000
REACTOME_CELL_CYCLE	48.00	0.47	3.88	0.00000	0.00000
REACTOME_CELL_CYCLE	48.00	0.47	3.79	0.00000	0.00000
BENPORATH_CYCLING_GENES	82.00	0.36	3.71	0.00000	0.00000
GO_CELL_CYCLE_PROCESS	91.00	0.34	3.70	0.00000	0.00000
REACTOME_CELL_CYCLE_MITOTIC	40.00	0.50	3.69	0.00000	0.00000
GO_CELL_CYCLE	108.00	0.31	3.60	0.00000	0.00000
HALLMARK_G2M_CHECKPOINT	27.00	0.57	3.55	0.00000	0.00000
REACTOME_DNA_REPLICATION	28.00	0.53	3.39	0.00000	0.00000
GO_REGULATION_OF_CELL_CYCLE	86.00	0.32	3.30	0.00000	0.00000
GO_MITOTIC_CELL_CYCLE	68.00	0.34	3.23	0.00000	0.00000
GO_DNA_REPLICATION	30.00	0.49	3.13	0.00000	0.00000
GO_CELL_CYCLE_PHASE_TRANSITION	31.00	0.49	3.12	0.00000	0.00000
GO_REGULATION_OF_CELL_CYCLE_PROCESS	48.00	0.37	3.02	0.00000	0.00014
REACTOME_MITOTIC_M_M_G1_PHASES	22.00	0.52	2.93	0.00000	0.00000
GO_CELL_DIVISION	39.00	0.40	2.90	0.00000	0.00022
GO_CELL_PROLIFERATION	61.00	0.32	2.85	0.00000	0.00019
REACTOME_G1_S_TRANSITION	16.00	0.59	2.80	0.00000	0.00006
REACTOME_MITOTIC_G1_G1_S_PHASES	19.00	0.54	2.78	0.00000	0.00006
REACTOME_S_PHASE	16.00	0.58	2.78	0.00000	0.00006
GO_CELL_CYCLE_G1_S_PHASE_TRANSITION	17.00	0.59	2.77	0.00000	0.00039
GO_REGULATION_OF_CELL_DIVISION	23.00	0.47	2.70	0.00000	0.00113
GO_REGULATION_OF_MITOTIC_CELL_CYCLE	46.00	0.34	2.68	0.00000	0.00116
REACTOME_SYNTHESIS_OF_DNA	14.00	0.58	2.55	0.00000	0.00062
BENPORATH_PROLIFERATION	22.00	0.46	2.54	0.00000	0.00062
GO_POSITIVE_REGULATION_OF_CELL_PROLIFERATION	66.00	0.28	2.52	0.00000	0.00309
KAUFFMANN_DNA_REPLICATION_GENES	21.00	0.45	2.49	0.00000	0.00098
WHITFIELD_CELL_CYCLE_S	24.00	0.42	2.44	0.00000	0.00135
REACTOME_CELL_CYCLE_CHECKPOINTS	13.00	0.57	2.43	0.00000	0.00137
GO_REGULATION_OF_CELL_PROLIFERATION	127.00	0.19	2.39	0.00000	0.00664
WHITFIELD_CELL_CYCLE_G1_S	22.00	0.40	2.25	0.00419	0.00447
KEGG_DNA_REPLICATION	10.00	0.58	2.24	0.00000	0.00470
REACTOME_M_G1_TRANSITION	10.00	0.58	2.21	0.00606	0.00545
WHITFIELD_CELL_CYCLE_G2_M	23.00	0.38	2.19	0.00000	0.00589
GO_REGULATION_OF_CELL_CYCLE_PHASE_TRANSITION	32.00	0.32	2.12	0.00200	0.01940
WHITFIELD_CELL_CYCLE_G2	29.00	0.32	2.07	0.00000	0.01143
GO_CELL_CYCLE_G2_M_PHASE_TRANSITION	14.00	0.42	1.90	0.01136	0.04134
HALLMARK_MITOTIC_SPINDLE	14.00	0.46	2.04	0.00189	0.01553
KEGG_CELL_CYCLE	16.00	0.40	1.87	0.01202	0.02866
FIRESTEIN_PROLIFERATION	13.00	0.38	1.64	0.03725	0.07637

*Mitotic G2-G2/M phases(R): GP4 (p=0, FDR<3.846e-05); GP2 (p=0.0097, FDR=0.06118).

*Mitotic Spindle: GP4 (P=0.0002, FDR=0.002811)

Supplementary Table 4. YAP1 targets are enriched in gene signatures associated with well known oncogenic signaling pathways and gene programs associated with squamous subtype of PDAC* (Bailey et al).

Validated targets of C-MYC transcriptional activation(N)*

NAME	SIZE	ES	NES	NOM p-val	FDR q-val
HALLMARK_TNFA_SIGNALING_VIA_NFKB	42	0.42	3.16	0.00000	0.00000
HALLMARK_MYC_TARGETS_V2	10	0.67	2.57	0.00000	0.00000
HALLMARK_MYC_TARGETS_V1	12	0.57	2.41	0.00000	0.00091
MYC_UP.V1_UP	14	0.45	2.06	0.00000	0.01826
DANG_BOUND_BY_MYC	71	0.28	2.69	0.00000	0.00017
DANG_MYC_TARGETS_UP	10	0.61	2.37	0.00000	0.00220
BILD_MYC_ONCOGENIC_SIGNATURE	23	0.39	2.30	0.00411	0.00350
ALFANO_MYC_TARGETS	24	0.32	1.82	0.01613	0.03544

*GP5 (P=0, FDR<1.000e-04), GP4 (P=0.0021,FDR=0.01989), GP2 (P=0.016, FDR=0.08453)

IL6-mediated signaling events(N)*

NAME	SIZE	ES	NES	NOM p-val	FDR q-val
CROONQUIST_IL6_DEPRIVATION_DN	23	0.64	3.60	0.00000	0.00000
DAUER_STAT3_TARGETS_UP	11	0.50	2.07	0.00382	0.01121
HALLMARK_IL6_JAK_STAT3_SIGNALING	11	0.39	1.62	0.04211	0.07865

*GP2 (P=0.0157, FDR=0.0835)

E2F transcription factor network(N)*

NAME	SIZE	ES	NES	NOM p-val	FDR q-val
HALLMARK_E2F_TARGETS	39	0.54	3.93	0.00000	0.00000
E2F1_UP.V1_UP	21	0.54	2.94	0.00000	0.00075
ISHIDA_E2F_TARGETS	13	0.58	2.56	0.00000	0.00058
PID_E2F_PATHWAY	14	0.51	2.33	0.00199	0.00275
BILD_E2F3_ONCOGENIC_SIGNATURE	32	0.31	2.08	0.00000	0.01104

*GP4 (P=0; FDR<4.762e-05)

RhoA signaling pathway(N)*

NAME	SIZE	ES	NES	NOM p-val	FDR q-val
BERENJENO_TRANSFORMED_BY_RHOA_UP	82	0.47	4.81	0.00000	0.00000

*GP3 (P=0.0029, FDR=0.02324)

TGFB/BMP Receptor Signaling*

NAME	SIZE	ES	NES	NOM p-val	FDR q-val
LEE_BMP2_TARGETS_DN	90	0.49	5.27	0.00000	0.00000
TGFB_UP.V1_UP	23	0.42	2.39	0.00000	0.00526
COULOUARN_TEMPORAL_TGFB1_SIGNATURE_UP	13	0.53	2.29	0.00000	0.00361
KARLSSON_TGFB1_TARGETS_UP	10	0.58	2.19	0.00199	0.00587
PLASARI_TGFB1_TARGETS_10HR_UP	36	0.29	1.93	0.00853	0.02192
MCBRYAN_PUBERTAL_TGFB1_TARGETS_UP	19	0.33	1.69	0.02863	0.06292

*BMP receptor signaling(N):GP3 (P=0.0001, FDR=0.001106)

TNF signaling pathway(K)*

NAME	SIZE	ES	NES	NOM p-val	FDR q-val
HALLMARK_TNFA_SIGNALING_VIA_NFKB	42	0.42	3.16	0.00000	0.00000
PHONG_TNF_TARGETS_UP	15	0.65	2.99	0.00000	0.00000

*GP2 (P= 0.0004; FDR=0.008161)

Supplementary Table 5. Yap1 targets in this study are enriched in Hippo signaling pathway (GP3) of squamous subtype (Bailey et al)

Bailey et al.	This study
Hippo signaling pathway(K) GP3_Reactome (p=0, FDR<7.692e-05)	**Pa04C-YAP^{S127A} (Fold Change)**
FZD10	128.00
WTIP	20.22
FGF10	12.90
TCF7L1	10.00
TGFB1	9.70
BMP8A	7.06
TGFBR1	6.80
BMP6	5.81
SMAD7	5.57
CTGF	3.28
TGFB3	2.80
LATS2	2.17
SNAI2	2.05
TEAD1	1.71
GLI2	0.49
FZD2	0.43
LEF1	0.10
DLG4	0.08

Supplementary Table 6. YAP1 signature: CORDENONSI_YAP_CONSERVED_SIGNATURE (GSEA MSigDB database)

AMOTL2
ANKRD1
AXL
BICC1
BIRC5
CDC20
CDKN2C
CENPF
COL4A3
CRIM1
CTGF
CYR61
DAB2
DDAH1
ASAP1
DLC1
DUSP1
DUT
ECT2
EMP2
ETV5
FGF2
FLNA
FSCN1
FSTL1
GADD45B
GAS6
GGH
GLS
HEXB
HMMR
AGFG2
ITGB2
ITGB5
LHFP
MARCKS
MDFIC
NDRG1
PDLIM2

PHGDH
PMP22
SCHIP1
SDPR
SERPINE1
SGK1
SH2D4A
SHCBP1
SLIT2
STMN1
TGFB2
TGM2
THBS1
TK1
TNNT2
TNS1
TOP2A
TSPAN3

Supplementary Table 7. Subtype signature genes used for NanoString analysis based on Collisson et al and Bailey et al studies (Nat Med. 2011, 17:500-3, Nature. 2016, 531:47-52)

Gene	Subtype	Source: Collisson	Source: Bailey
TNC	Squamous	0	1
PTHLH	Squamous	0	1
TMEM40	Squamous	0	1
KLC3	Squamous	0	1
CAV1	Squamous	1	1
TGFBI	Squamous	0	1
GJB6	Squamous	0	1
CDH26	Squamous	0	1
EREG	Squamous	0	1
RHCG	Squamous	0	1
RGS20	Squamous	0	1
GSDMC	Squamous	0	1
HMGA2	Squamous	0	1
C16orf74	Squamous	0	1
IVL	Squamous	0	1
A2ML1	Squamous	0	1
NIPAL4	Squamous	0	1
KRT5	Squamous	0	1
KRT14	Squamous	1	1
RFX8	Squamous	0	1
S100A2	Squamous	1	1
L1CAM	Squamous	0	1
KRT6A	Squamous	0	1
MIR205HG	Squamous	0	1
TWIST1	Squamous	1	0
NT5E	Squamous	1	0
PMAIP1	Squamous	1	0
LOX	Squamous	1	0
SLC2A3	Squamous	1	0
GPM6B	Squamous	1	0
PAPPA	Squamous	1	0
AIM2	Squamous	1	0
TFF1	Progenitor	1	1
CEACAM5	Progenitor	1	0
TFF3	Progenitor	1	0
ATP10B	Progenitor	1	1
CAPN8	Progenitor	1	1
CEACAM6	Progenitor	1	0
TSPAN8	Progenitor	1	1
TOX3	Progenitor	1	1
GPX2	Progenitor	1	1
SDR16C5	Progenitor	1	0
PHGR1	Progenitor	0	1
DPCR1	Progenitor	0	1
SEMG1	Progenitor	0	1
SLC9A3	Progenitor	0	1
SULT1B1	Progenitor	0	1

FAM177B	Progenitor	0	1
MUC17	Progenitor	0	1
CAPN9	Progenitor	0	1
EDN3	Progenitor	0	1
CLDN18	Progenitor	0	1
MYO7B	Progenitor	0	1
BTNL8	Progenitor	0	1
IHH	Progenitor	0	1
CELA3A	ADEX	1	1
CTRB2	ADEX	1	1
PLA2G1B	ADEX	1	1
REG1B	ADEX	1	1
CELA3B	ADEX	1	1
CLPS	ADEX	1	1
CEL	ADEX	1	1
PRSS1	ADEX	1	1
GP2	ADEX	1	1
CTRB1	ADEX	0	1
SYCN	ADEX	0	1
CPA2	ADEX	0	1
CPA1	ADEX	0	1
REG3G	ADEX	0	1
CTRC	ADEX	0	1
AQP8	ADEX	0	1
CUZD1	ADEX	0	1

Supplementary Table 8. KRAS-independent signature based on Kapoor et al, Cell. 2014. 158 (1): 185-197

RECQL
CAV1
RGS10
IFIT2
WWP2
CXCL12
TGFBI
CCDC122
IMPACT
PCDH19
EVC
EVC2
COL6A2
SLC24A3
GXYLT2
GKAP1
TBX18
AFAP1L2
PREX2
ZFPM2
WISP1
DHX58
C11orf70
SHOX2
CXCL2
ZNF33A
NRG1
CXCL10
GPR176
EYA4
PYCR1
MEF2C
ADH7
CSF1
MAOA
OGN
TBX15
CLSTN2
MX2
COL5A2
RRAD
PARP12
GBP3
DCN
OMD
IFI44
ARMCX2
WISP2
IRAK1BP1

COL1A2
BIRC3
TGFB2
ASPN
ZBP1
GLI3
EMILIN1
BIRC2
CSPG4
FNDC4
PAK3
PTN
SFRP2
FHL1
TMEM140
FAM13C
RTP4
DDR2
BNC2
COL1A1
RCN1
PDGFRB
MGST1
FGF7
PKIA
SERPINE1
HPGD
XAF1
ALDH1L2
BST2

Supplementary Table 9. Non-canonical WNT signature: PID_WNT_NONCANONICAL_PATHWAY (GSEA MSigDB database)

ARRB2
CAMK2A
CDC42
CHD7
CSNK1A1
CTHRC1
DAAM1
DVL1
DVL2
DVL3
FLNA
FZD2
FZD5
FZD6
FZD7
MAP3K7
MAPK10
MAPK8
MAPK9
NFATC2
NLK
PPARG
PRKCZ
RAC1
RHOA
ROCK1
ROR2
SETDB1
TAB1
TAB2
WNT5A
YES1